Received: 25 October 2016 | Revised: 23 December 2017 | Accepted: 4 January 2018

DOI: 10.1111/geb.12724

RESEARCH PAPER

WILEY Global Ecology and Biogeography A Journal of Macroecology

Reconstructing deep-time palaeoclimate legacies in the clusioid Malpighiales unveils their role in the evolution and extinction of the boreotropical flora

Andrea S. Meseguer[1,2,3] | Jorge M. Lobo[4] | Josselin Cornuault[1] | David Beerling[5] | Brad R. Ruhfel[6,7] | Charles C. Davis[7] | Emmanuelle Jousselin[2] | Isabel Sanmartín[1]

[1]Department of Biodiversity and Conservation, Real Jardín Botánico, RJB-CSIC, Madrid, Spain

[2]INRA, UMR 1062 CBGP (INRA, IRD, CIRAD, Montpellier SupAgro), The Center for Biology and Management of Populations (CBGP), Montferrier-sur-Lez, France

[3]CNRS, UMR 5554 Institut des Sciences de l'Evolution (Université de Montpellier), Montpellier, France

[4]Department of Biogeography and Global Change, Museo Nacional Ciencias Naturales, MNCN-CSIC, Madrid, Spain

[5]Department of Animal and Plant Sciences, University of Sheffield, Sheffield, United Kingdom

[6]Department of Biological Sciences, Eastern Kentucky University, Richmond, Kentucky

[7]Department of Organismic and Evolutionary Biology, Harvard University Herbaria, Cambridge, Massachusetts

Correspondence
Andrea S. Meseguer CNRS, UMR 5554 Institut des Sciences de l'Evolution (Universite de Montpellier), Montpellier, France.
Emails: asanchezmeseguer@gmail.com

Funding information
Spanish Government, Grant/Award Number: AP-2007-01698, CGL2009-13322-C01, CGL2011-25544, CGL2012-40129-C01, CGL2015-67849-P (MINECO/FEDER); AgreenSkills, Grant/Award Number: 26719; CEBA, Grant/Award Number: ANR-10-LABX-25-01; Marie-Curie Actions, Grant/Award Number: MSCA-IF-EF-ST-708207

Abstract

Aim: During its entire history, the Earth has gone through periods of climate change similar in scale and pace to the warming trend observed today in the Anthropocene. The impact of these ancient climatic events on the evolutionary trajectories of organisms provides clues on the organismal response to climate change, including extinction, migration and persistence. Here, we examine the evolutionary response to climate cooling/warming events of the clusioid families Calophyllaceae, Podostemaceae and Hypericaceae (CPH clade) and the genus *Hypericum* as test cases.

Location: Holarctic.

Time period: Late Cretaceous–Cenozoic.

Major taxa studied: Angiosperms.

Methods: We use palaeoclimate simulations, species distribution models and phylogenetic comparative approaches calibrated with fossils.

Results: Ancestral CPH lineages could have been distributed in the Holarctic 100 Ma, occupying tropical subhumid assemblages, a finding supported by the fossil record. Expansion to closed-canopy tropical rain forest habitats occurred after 60 Ma, in the Cenozoic, in agreement with earlier ideas of a post-Cretaceous origin of current tropical rain forest. Posterior Cooling during the Eocene triggered diversification declines in CPH tropical lineages, and was associated with a climatic shift towards temperate affinities in *Hypericum*. *Hypericum* subsequently migrated to tropical mountains, where it encountered different temperate conditions than in the Holarctic.

Main conclusions: We hypothesize that most clusioid CPH lineages failed to adapt to temperate regimes during periods of Cenozoic climate change, and went extinct in the Holarctic. In contrast, boreotropical descendants including *Hypericum* that underwent niche evolution demonstrated selective advantages as climates became colder. Our results point toward macroevolutionary trajectories involving the altering fates of closely related clades that adapt to periods of global climate change versus those that do not. Moreover, they suggest the hypothesis that potentially many clades, particularly inhabitants of boreotropical floras, were likely extirpated from the Holarctic and persist today (if at all) in more southern tropical locations.

KEYWORDS

boreotropical flora, climate cooling, diversification, fossils, *Hypericum*, niche evolution

1 | INTRODUCTION

Climate change is a major agent driving species distribution and diversity patterns (Svenning, Eiserhardt, Normand, Ordonez, & Sandel, 2015). Often, studies on biotic impacts of climate change focus on species' demographic responses to recent climatic oscillations (Hewitt, 2000), or the effect of current global warming on biodiversity loss (Dawson, Jackson, House, Prentice, & Mace, 2011). Yet, short temporal scales might be limited in their capacity to predict the long-term effects of climatic oscillations. The Earth's past climate has gone through periods of climate change that are similar in scale and pace to the warming trend we observe today during the Anthropocene (Zachos, Dickens, & Zeebe, 2008). Disentangling the response of organisms to these ancient climatic events is key to understanding the impact of current warming on biodiversity, but requires the combination of multiple data layers (Svenning et al., 2015), including inferences on the timing of past diversification events, and the palaeoclimatic and geographical context under which they occurred. Extinction is likely to have removed important parts of a lineage's evolutionary history, adding uncertainty. Including fossil information is thus important in deep-time ancestral inferences (Betancur-R, Ortí, & Pyron, 2015; Meseguer, Lobo, Ree, Beerling, & Sanmartin, 2015; Slater, Harmon, & Alfaro, 2012). Available palaeoclimate data are often restricted to the recent past (Otto-Bliesner, Marshall, Overpeck, Miller, & Hu, 2006), limiting also our ability to infer the impact of ancient events. As a result, studies on deep-time palaeoclimate legacies on biodiversity remain scarce (Svenning et al., 2015).

Dramatic events of climate change occurred during the last *c.* 100 Myr. The Late Cretaceous is considered a warm period that culminated with the mass extinction of the Cretaceous–Palaeogene boundary (K-Pg; 66 Ma) and the impact winter brought by the K-Pg event (Huber, Norris, & MacLeod, 2002; Wilf, Johnson, & Huber, 2003; Zachos et al., 2008). After the K-Pg, climates were relatively cool until the late Palaeocene–early Eocene, when global temperatures increased again. They reached a (Cenozoic) maximum during the Early Eocene Climate Optimum (EECO), 53–51 Ma, when temperatures became *c.* 10 degrees warmer than present (Beerling, Fox, Stevenson, & Valdes, 2011; Zachos et al., 2008), and warm, frost-free, equable climates extended over the northern and southern latitudes (Morley, 2000; Ziegler et al., 2003). By the Late Eocene (*c.* 34 Ma), a precipitous drop in global temperatures, termed the Terminal Eocene Event (TEE; Meyer & Manchester, 1997; Wolfe, 1992), intensified the global cooling trend that started in the Cretaceous and climaxed during the Pleistocene glaciations. This trend was punctuated with other cooling and warming periods such as the Late Miocene Cooling (LMC; Beerling, Berner, Mackenzie, Harfoot, & Pyle, 2009), the Middle Miocene Climate Optimum (MMCO, *c.* 17–15 Ma) or the Mid Pliocene Warming Event (MPWE, 3.6 Ma; Willis & MacDonald, 2011; Zachos et al., 2008).

The fossil record indicates that these climatic changes were accompanied by concomitant changes in vegetation. The greenhouse interval of the Eocene promoted the extension of tropical rain forest habitats in the equator (Johnson & Ellis, 2002; Wing et al., 2009) and warm paratropical assemblages in northern latitudes, the so-called *boreotropical* vegetation, at the expense of the subhumid forests of the Late Cretaceous (Morley, 2000; Wing et al., 2012; Ziegler et al., 2003). Conversely, the TEE global cooling led in the Holarctic to a transition from the *boreotropical* vegetation (broad-leaved evergreen and hardwood deciduous taxa) to a *mixed-mesophytic forest* composed by more mesic warm temperate elements (Morley, 2007; Tiffney, 1985; Wolfe, 1975).

At the lineage level, palaeontological and phylogenetic evidence suggests that the response of plants to these climatic events was diverse, including extinction (Antonelli & Sanmartín, 2011; Pokorny et al., 2015; Xing, Onstein, Carter, Stadler, & Linder, 2014); migration (Couvreur et al., 2011; Davis, Bell, Mathews, & Donoghue, 2002; Morley, 2007), or persistence and adaptation, with the evolution of new climatic preferences and relevant traits (Willis & MacDonald, 2011). In the case of the TEE, the latter would have required the evolution of complex physiological systems to cope with frost, such as shedding leaves during freezing periods or senescing above-ground tissues (Zanne et al., 2014). Although there is phylogenetic evidence that adaptation to cold has occurred several times in angiosperms (Donoghue & Edwards, 2014; Spriggs et al., 2015), evidence for the EECO–TEE boreotropical/temperate vegetation transition comes mainly from the palaeobotanical literature (Tiffney, 1985; Wolfe, 1977).

The clusioid clade, in the order Malpighiales (Wurdack & Davis, 2009; Xi et al., 2012), provides an excellent test case to explore the response of flowering plants to rapid climate change, including episodes of global warming (EECO) and cooling (TEE). This clade includes five families, Bonnetiaceae, Calophyllaceae, Clusiaceae, Podostemaceae and Hypericaceae, comprising *c.* 1900 species, and 94 genera (Ruhfel et al., 2011; Figure 1). Molecular evidence indicates that these families radiated in a rapid burst during the Late Cretaceous (Ruhfel, Bove, Philbrick, & Davis, 2016; Xi et al., 2012), while ancestral niche reconstructions (Davis, Webb, Wurdack, Jaramillo, & Donoghue, 2005) place their ancestors as early members of the tropical rain forest biome. Today, clusioid families occur in a variety of habitats including closed-canopy rain forests, dry tropical vegetation, temperate forests, and aquatic environments (Stevens, 2007). The majority of clusioid species, however, inhabit the tropical regions of South America, Africa and Southeast Asia, except species of *Hypericum* (St John's wort, Hypericaceae), the most diverse clusioid genus, *c.* 500 species (Robson, 2012), and the only one that has achieved a nearly cosmopolitan distribution across the temperate regions of the world and tropical mountains of the Southern Hemisphere (Meseguer, Aldasoro, & Sanmartin, 2013).

Previous studies have suggested a link between the evolutionary success of *Hypericum* and the evolution of new temperate affinities relative to their clusioid ancestors (Meseguer et al., 2013, 2015; Nürk, Uribe-Convers, Gehrke, Tank, & Blattner, 2015). A recent work placed this event of niche evolution in the Oligocene, concomitant with climate cooling and initial diversification in the genus (Nürk et al., 2015). However, phylogenetic and climatic inference in this study did not go further back than the stem-node of *Hypericum* – the divergence between tribe Hypericeae (= *Hypericum*) and tropical sister tribes Vismieae and Cratoxyleae. This limited the ability to explicitly test the niche evolution hypothesis, as information prior to the crown node of Hypericaceae was missing, introducing uncertainty in the inference of

FIGURE 1 Growth form, morphological, and ecological diversity in the clusioid Calophyllaceae, Podostemaceae and Hypericaceae (CPH) clade. (a) *Apinagia flexuosa*, (b) *Mourera fluviatilis*, (c) *Castelnavia* sp., (d) *Hypericum elodes*, (e) *Hypericum revolutum*, (f) *Mammea americana*, (g) *Kielmeyera* sp., (h) *Kielmeyera* sp., (i) *Kielmeyera* sp., (j) *Hypericum richeri*. Photographs by B. Ruhfel. *Hypericum* photos by A.S. Meseguer. *H. elodes* photo from www.aphotoflora.com

ancestral climatic preferences. In addition, fossil evidence suggests that some clusioid lineages were present in the Holarctic before the TEE transition: that is, Late Cretaceous fossil record of Clusiaceae from North America (Crepet & Nixon, 1998) and Palaeogene pollen of *Calophyllum* (Calophyllaceae) from Europe (Cavagnetto & Anadón, 1996). At the start of the Mid Cenozoic, however, these families disappear entirely from the fossil record of the northern latitudes. What might explain that disappearance from high latitudes?

Here, we use fossil information in combination with palaeoclimate data, species distribution models (SDMs) and macroevolutionary inference methods calibrated with fossils to reconstruct ancestral climatic preferences, past geographical distributions, and diversity dynamics in *Hypericum* and its closest clusioid relatives: genera within the clade of families (Callophylaceae (Podostemaceae, Hypericaceae)), herein the clusioid CPH clade. Specifically, our aim is to address the following questions: (a) Were the ancestors of the clusioid CPH clade adapted to tropical conditions? (b) Is there support for a geographical distribution of CPH lineages in the Holarctic during the Late Cretaceous–Early Cenozoic? (c) When did the modern temperate climatic preferences of *Hypericum* evolve, and have these preferences been conserved over time? (d) Is there a link between the acquisition of temperate affinities and the evolutionary success of *Hypericum* (wider distribution, higher number of species) compared with other clusioid CPH lineages?

2 | METHODS

2.1 | Reconstructing ancestral niche and past geographical distributions

2.1.1 | Compilation of distributional and climatic data

Extant distributional data for the clusioid CPH clade were obtained from online databases (http://www.gbif.org, accessed January 2017) and from our own collection. A total of 173,459 data points were collated to exclude ambiguous citations (points in the sea, country centroids, areas out of the native distribution of the species) and repeated occurrences using *SpeciesGeoCoder* (Töpel et al., 2017); manual verification was also necessary, as this software did not eliminate all ambiguities. The final dataset included 48,467 occurrences in cells of 5 arcminutes for Hypericaceae (representing six genera and 480 Hypericeae spp. out of 612 described in the family), Podostemaceae (590 occurrences for 38 genera/145 spp. out of 306) and Calophyllaceae (4,697 occurrences, 15 genera/276 spp. out of 478) (Supporting Information Appendix S1). Fossil data (14 records from the Late Eocene to the Oligocene; Supporting Information Appendix S2) were obtained from the literature (Meseguer & Sanmartín, 2012; Meseguer et al., 2015). A detailed discussion on the fossil record of *Hypericum* from Meseguer et al. (2015) can be found in Supporting Information Appendix S3.

Current climatic data were obtained from WorldClim (Hijmans, Cameron, Parra, Jones, & Jarvis, 2005) at a resolution of 5 arc-minute cells. For past scenarios we used Hadley Centre coupled ocean–atmosphere general circulation models, at a resolution of 2.5° × 3.75°, excepting the Cretaceous layer at a resolution of 5° × 5° (Beerling et al., 2009, 2011), which represent six major global warming/cooling events in the Earth's recent history, and are designed to incorporate the effects of changing levels of atmospheric CO_2: (a) Turonian (Cretaceous) (representing the geology and palaeotectonics of the time interval 93–89 Ma, and modelled under 1120 ppm CO_2), (b) EECO (53–51 Ma, 1120 ppm CO_2); (c) TEE (34 Ma, 560 ppm); (d) MMCO (17–14 Ma, 400 ppm); (e) LMC (11.6 Ma, 280 ppm); (f) MPWP (3.6 Ma, 560 ppm); and (g) the Preindustrial world (> 1900s, 280 ppm). The last five were used in Meseguer et al. (2015). The Turonian palaeoclimate model is here used for the first time to accommodate potential climate change during the early history of the clusioid clade. These palaeoclimate models include average monthly temperature and precipitation values and were used here to generate seven climatic variables: annual precipitation (AP), annual variation in precipitation (AVP), maximum monthly precipitation (MXMP), minimum monthly precipitation (MNMP), mean annual temperature (MAT), maximum monthly temperature (MXMT) and minimum monthly temperature (MNMT). Among these, we selected the four showing iteratively a variance inflation factor (VIF) lower than 5: AP, MNMP, MNMT and MXMT. VIF quantifies the multicollinearity of predictors (Dormann et al., 2013), and a value of 5 indicates that the selected predictors are only moderately correlated.

2.1.2 | Ancestral niche reconstruction

To reconstruct ancestral climatic preferences, we used a composite phylogenetic hypothesis representing relationships at the genus level within the CPH clade and at the section level within *Hypericum* (methods used to construct these trees are described in Supporting Information Appendix S3). The clusioid tree was obtained from Ruhfel et al. (2016)'s study and represents 76 of the 94 described clusioid genera, covering all major morphological and biogeographical variation in the group (see Figure S4.1 in Supporting Information Appendix S4'). The tree was pruned, using *ape* (Paradis, Claude, & Strimmer, 2004), to include only representatives of the CPH clade. The *Hypericum* dated tree was obtained from the species-level phylogeny of Meseguer et al. (2015), which includes 114 species, and represents all recognized major geographical and morphological variation (Supporting Information Figure S4.2). Because representation of species within sections in this tree was uneven and to avoid bias in the ancestral inference of climatic niches (i.e. different number of tips across *Hypericum* sections and clusioid lineages), we pruned the *Hypericum* tree to include one species per major clade recognized by Meseguer et al. (2013) (Table S5.1 in Supporting Information Appendix S5). Similarly, some genera recovered as non-monophyletic in the CPH clusioid clade (Ruhfel et al., 2011) were collapsed to the same branch (see Supporting Information Table S5.2). The *Hypericum* tree was grafted into the clusioid tree using the function *bind.tree* in *ape*, with a branch length proportional to the age recovered for the crown age of *Hypericum* (Meseguer et al., 2015), which is congruent with the one obtained by Ruhfel et al. (2016) (Supporting Information Figures S4.1 and S4.2). The final supertree included 42 tips, representing all major geographical, phylogenetic and morphological variation in families Calophyllaceae, Podostemaceae and Hypericaceae.

We estimated climatic preferences at the nodes of the clusioid CPH tree using continuous-trait ancestral state inference models (O'Meara, 2012), implemented in the Bayesian software RevBayes (Höhna, Landis et al., 2016), and based on a Brownian model of niche evolution. For each climatic variable, tip values were calculated as the centroid of the climatic conditions of all occurrences assigned to the tip: (max + min)/2. Fossil information was included for *Hypericum* (Late Eocene) crown-ancestors, calculated as the centroid of the climatic condition of Eocene–Oligocene *Hypericum* fossil occurrences in the Late Eocene (560 ppm) simulation (Supporting Information Table S5.3). The position of this fossil calibration was let as a free parameter along the stem branch of *Hypericum* and integrated upon. We tested the impact of calibration on our estimates by considering all models with and without calibration.

We initially considered more adaptive models, such as the Ornstein-Uhlenbeck OU or multiple OU models (O'Meara, 2012). However, the selective optimum and the root state cannot be identified under the OU model (Ho & Ané, 2014). We found that this effect concerned all ancestral trait estimates when fitting the OU model on simulated datasets, with highly negatively correlated posterior samples of the selective optimum and ancestral traits. Ho and Ané (2014) further showed that this problem generalizes to multiple-optima OU models. Finally, extensive tests for the fitting of OU models in RevBayes (Cornuault, in prep.) revealed that the inferred number of selective regimes in a multiple-optima OU model, or the uncertainty associated with ancestral trait estimates, are highly dependent on the choice of prior for the selection strength parameter of the OU model. In contrast, ancestral traits were generally estimated accurately and with higher precision using a Brownian model, even for data generated under strong OU models (Cornuault, in prep.). Considering these problems with the inference of ancestral traits using OU models, we decided to use the Brownian model.

For the Brownian model, we relaxed the hypothesis of a constant rate of niche evolution by using an uncorrelated exponential relaxed clock for niche traits. Specifically, each branch received its own rate, assumed to be exponentially distributed, with mean μ_σ:

$$\sigma_i \sim exponential(1/\mu_\sigma) \quad (1)$$

The average rate μ_σ then received an exponential prior of mean 10:

$$\mu_\sigma \sim exponential(1/10) \quad (2)$$

This prior was much flatter than the posterior in all analyses, so it is effectively uninformative relative to the likelihood.

Tip traits were scaled to mean 0 and unit variance before analysis and the root trait received a normal prior with high variance (100) relative to that of tip traits (1):

$$t_r \sim normal(0,10) \quad (3)$$

The trait value at the end of branch *i*, t_i, received the Brownian motion distribution:

$$t_i \sim normal(t_{a(i)}, \sigma_i \sqrt{b_i}) \quad (4)$$

where b_i is the length of branch *i*, and *a(i)* denotes the index of the ancestor of branch *i*.

The time of calibration received a uniform prior between τ_s and τ_e, the starting and ending times of the calibration branch (i.e. the stem of *Hypericum*):

$$\tau_c \sim uniform(\tau_s, \tau_e) \quad (5)$$

The calibration branch was cut in two parts, with:

$$t_c \sim normal(t_{a(k)}, \sigma_k \sqrt{(b_k - (\tau_c - \tau_s))}) \quad (6)$$

$$t_k \sim normal(t_c, \sigma_k \sqrt{(b_k - (\tau_e - \tau_c))}) \quad (7)$$

where *k* is the index of the calibration branch and t_c is the trait calibration value (fixed).

This model was implemented in RevBayes and three independent runs of 100,000 iterations were carried out with a thinning of 10, providing a final sample of size 30,000 for temperature variables (scripts are available in Supporting Information Appendix S6). The posterior distributions of models for precipitation variables were a posteriori conditioned on ancestral traits being positive, by removing all iterations with at least one negative ancestral trait value. This procedure left 29,874 and 19,608 posterior samples for the AP and MNMP variables, respectively. Each Markov chain Monte Carlo (MCMC) run was initially burnt-in for 10,000 iterations, comprising a period of warm-up (wherein operator parameters were tuned) of 5,000 iterations.

To answer question (b) in the Introduction on whether clusioids were distributed in the Holarctic before the TEE, we represent the potential distribution of major ancestral clusioid CPH lineages by transferring the reconstructed climatic values of each node [with ancestral state reconstruction (ASR)] to the corresponding palaeoclimate simulation. The four climatic variables previously selected and the scale-invariant Mahalanobis distance (MD) were used to calculate the climatic distance of each cell from the hypothetical 'climatic optima' represented by the reconstructed climatic values of each node. The lower quartile of the so obtained MD values was used to represent the most suitable areas.

2.1.3 | Diversification analyses

To investigate the impact of climate cooling on diversification trajectories in the clusioid CPH clade and answer question (d) in the introduction on whether a change in climatic preferences triggered rapid diversification in *Hypericum*, we inferred rates of lineage diversification using stochastic birth-death models and Bayesian MCMC methods in the R package TESS (Höhna, May, & Moore, 2016). The supertree described above was used to explore diversification dynamics within the CPH clusioid clade, while for *Hypericum* we used the species-level tree from Meseguer et al. (2015), which allowed us to go deeper into diversification patterns within sections of *Hypericum*. TESS allows comparison among various diversification regimes, including birth-death models where speciation and extinction rates are constant, vary continuously over time, or change episodically in time (CoMET model). In the latter, speciation and extinction are allowed to change at discrete intervals, while including also explicit models for mass-extinction (global sampling) events (May, Höhna, & Moore, 2016). For the clusioid tree, incomplete taxon sampling was accommodated using the 'diversified' strategy in TESS, which is appropriate when sampling is intended to include representatives of major clades, for example clusioid genera (Höhna, May et al., 2016). For *Hypericum*, we used uniform random sampling with probability p = 0.3. A constant-rate model was specified with two parameters, the speciation and extinction rate, each controlled by an exponential prior distribution with rate = 0.1. We also tested four models with continuously varying diversification rates, in which speciation and extinction rates decrease or increase exponentially over time, while the other parameter remains constant. We used exponential priors for all parameters as above (scripts are available in Supporting Information Appendix S6). For all models, we ran two MCMC chains for one million iterations each (function *tess.mcmc*), thinning every 100th and discarding the first 1,000 as burnin, and using the auto-tuning function. We used the package coda (Plummer, Best, Cowles, & Vines, 2006) to summarize samples and assess good mixing (ESS > 200) of MCMC runs. The Gelman–Rubin test (Gelman & Rubin, 1992) was used to evaluate convergence among runs. Finally, we used stepping-stone simulations to estimate the marginal likelihood of the data under each model described above (with 1000 iterations and 50 power posteriors), and compare these using Bayes factors. Because the number of possible episodic models is infinite, we first used reversible-jump MCMC (rjMCMC) approaches in CoMET (*tess.analysis*) to integrate model uncertainty over all possible episodically varying birth-death processes including time of rate shifts and mass-extinction events (May et al., 2016). The function *empiricalHyperPriors* = TRUE was used to determine the form of the hyperpriors for the diversification parameters (speciation and extinction rate changes and mass-extinction events). We then ran the episodic (CoMET) model with *tess.mcmc*, with the number of rate shifts fixed to those estimated with rjMCMC; the marginal likelihood was estimated by stepping-stone and this value compared to the other models by Bayes factors.

3 | RESULTS

3.1 | Ancestral niche reconstruction

Supporting Information Table S5.4 shows extant climatic preferences for clusioid CPH lineages and *Hypericum* clades. Supporting Information Appendices S7–S14 show for each variable the inferred climatic values with or without fossil calibrations. The ancestor of the CPH clade was found to have lived under similar temperature and precipitation conditions to current tropical non-*Hypericum* Hypericaceae and Podostemaceae taxa (Figure 2; Supporting Information Figure S4.3). The ancestors of Calophyllaceae species thrived under similar temperature but higher precipitation regimes (AP and MNMP) than most other CPH lineages. Stem-node *Hypericum* was estimated to occur in tropical conditions (similar to other non-*Hypericum* Hypericaceae and Podostemaceae taxa), while the ancestral niches within the *Hypericum* clade were

Global Ecology and Biogeography
A Journal of Macroecology

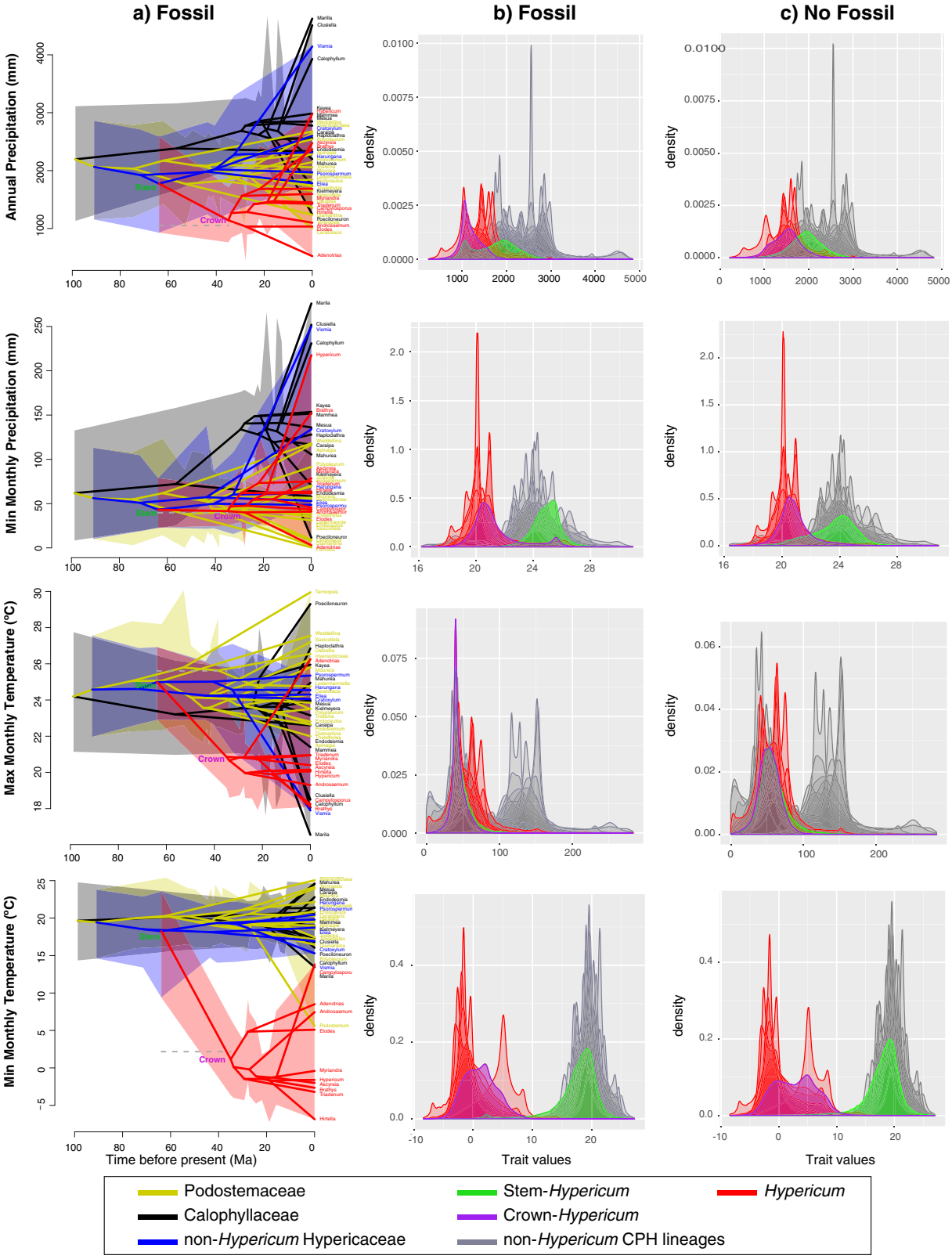

FIGURE 2 (a) Traitgrams showing the inferred evolution of climatic variables (annual precipitation, minimum monthly precipitation, minimum and maximum monthly temperature) using fossil calibrations and over the dated phylogenetic tree of the clusioid Calophyllaceae, Podostemaceae and Hypericaceae (CPH) clade in a space defined by the phenotype (*y* axis). Shaded areas encompass all HPD intervals of the group concerned. The grey dashed horizontal line represents the fossil calibration value. (b) Posterior distributions of ancestral traits estimated for all nodes using fossil calibrations. (c) Posterior distributions of ancestral traits estimated for all nodes based on present taxa only

characterized by lower temperatures, especially for the MNMT, and precipitation regimes (Figure 2). The Bayesian posterior distribution of the difference between average trait values for all most recent common ancestors (MRCAs) of *Hypericum* clades (including crown node) and the values estimated for stem-*Hypericum* node yielded 95% highest posterior density (HPD) intervals larger than 0 for the temperature variables, but were non-significant for precipitation variables (Supporting Information Figure S4.4). We also calculated the difference between average reconstructed values for all *Hypericum* MRCAs and the average MRCAs of other non-*Hypericum* species in the tree, and found that the HPD for the difference is below 0 for all variables, except for MNMP, which did not differ between the two groups. Finally, we found no difference in trait values between the stem-*Hypericum* node and the average MRCA of other CPH clusioid taxa for all variables. In sum, our fossil-informed analyses support with confidence that *Hypericum* crown ancestors have on average lower temperature and precipitation (more temperate) values than the rest of the tree. The analyses without fossil constraints produced similar results (Supporting Information Figure S4.3), although differences between average *Hypericum* trait values and stem-*Hypericum* were smaller (Supporting Information Figure S4.5) – living under slightly wetter (AP) and warmer regimes (MNMT) – and uncertainty was slightly higher for stem-*Hypericum* reconstructions (Figure 2).

The geographical projection of these ancestral climatic values onto the corresponding palaeoclimate layer (Figure 3) indicates that the ancestors of CPH lineages could have found favourable conditions in the (presently) tropical regions of northern South America and central Africa, the southern coasts of the Northern Hemisphere, and the East Gondwana landmasses of Antarctica, southern South America, and Australia. The geographical extent of these favourable conditions increased in the Holarctic for the ancestors of family Hypericaceae, whereas *Hypericum* shows a continuous presence across the southern parts of the Northern Hemisphere during the entire Cenozoic period, in agreement with projections obtained from fossil-based SDMs (Meseguer et al., 2015).

3.2 | Diversification analyses

For *Hypericum*, the episodic diversification model fitted the data slightly better than the constant rate model Bayes Factor (BF > 1.3), but substantially better than other continuous-varying diversification models (BF > 6.7; Supporting Information Table S5.5). CoMET (TESS) did not find evidence of mass extinctions in *Hypericum*, but identified a rate shift (weakly supported) towards increasing speciation and decreasing extinction around 15–10 Ma (BF = 2; Figure 4; Supporting Information Figure S4.6). For the clusioid tree, the constant-rate model fitted the data slightly better than a model with extinction increasing over time (*lncrD*, BF= 1.2) and than the episodic model (BF = 2.2). The latter identified a supported shift (BF > 4) towards decreasing speciation rates during the Late Eocene–Miocene, between 30 and 10 Ma (Figure 4; Supporting Information Figure S4.7). The lack of significant support (BF > 5) for varying diversification rates in our models is likely a result of the small tree size. In any case, for the clusioids, models showing an increase in extinction rates were strongly preferred (BF > 10; Supporting Information Table S5.6) over all models with varying speciation and constant extinction.

4 | DISCUSSION

4.1 | Late Cretaceous–early Cenozoic evolution of the clusioid CPH clade: climate-driven extinction and southward migration

Fossil evidence suggests that most Late Cretaceous floras were tropical-like but largely represented by open and subhumid vegetation (Upchurch & Wolfe, 1987; Wing et al., 2012). The most accepted view is that the tropical, closed-canopy rain forest originated more recently, following the impact winter precipitated by the K-Pg mass extinction (Jaramillo et al., 2010; Johnson & Ellis, 2002; Morley, 2000; Wing et al., 2009). Controversy, however, exists in this regard, with some evidence suggesting that wet-megathermal forest, including angiosperms, arose by the Cenomanian, before the K-Pg (Boyce, Lee, Field, Brodribb, & Zwieniecki, 2010; Davis et al., 2005; Wolfe & Upchurch, 1987).

Based on current species habitat occupancy, Davis et al. (2005) reconstructed the habitat of the ancestral species of the clusioid clade (*c.* 102 Ma; Supporting Information Figure S4.1; Ruhfel et al., 2016) in warm, wet, closed-canopy forests. This reconstruction, however, did not include representatives of family Calophyllaceae, so the habitat occupancy of the CPH clade (*c.* 99 Ma) could not be fully inferred. Yet, ancestors of Podostemaceae + Hypericaceae (*c.* 91 Ma) were inferred to have lived under drier conditions than the clusioid ancestor, in open-canopy, dry tropical vegetation (Davis et al., 2005). Our palaeoclimatic reconstructions based on the inference of ancestral climatic preferences suggest that the Cenomanian clusioid ancestors – in this case the CPH clade – occupied warm subhumid assemblages. Specifically, we inferred that the MRCA of Calophyllaceae, Podostemaceae and Hypericaceae lived during the Late Cretaceous in regions with similar temperatures but drier precipitation regimes (AP = 2000 mm) than more recently evolved tropical Calophyllaceae (AP = 4000 mm), although in similar regions than those inhabited by most extant Podostemaceae and Hypericaceae species (Figure 2). The evolution of preferences for more humid environments in the CPH clade is estimated to have evolved later, during the early Cenozoic (< 60 Ma), and independently in families Calophyllaceae and Hypericaceae, in agreement with a post K-Pg origination of the tropical rain forest biome. We acknowledge, however, that we are considering very large geographical areas, which likely encompass high variability in habitats, and that there is fossil evidence from North America suggesting the presence of tropical rain forests before the K-Pg (Wolfe & Upchurch, 1987).

These findings have additional implications for the fossil *Paleoclusia chevalieri* (90 Ma) from New Jersey (Crepet & Nixon, 1998). As a close relative of the CPH clade – placed within the clusioid clade as stem or crown member of Clusiaceae s.s. (Ruhfel, Stevens, & Davis, 2013) – our results raise the possibility that this taxon inhabited warm-subhumid habitats in the Holarctic during the Late Cretaceous as well. This is supported by its Northern Hemisphere distribution, similar to CPH ancestors (Figure 3), and by earlier interpretations of the New Jersey locality

Global Ecology and Biogeography
A Journal of Macroecology

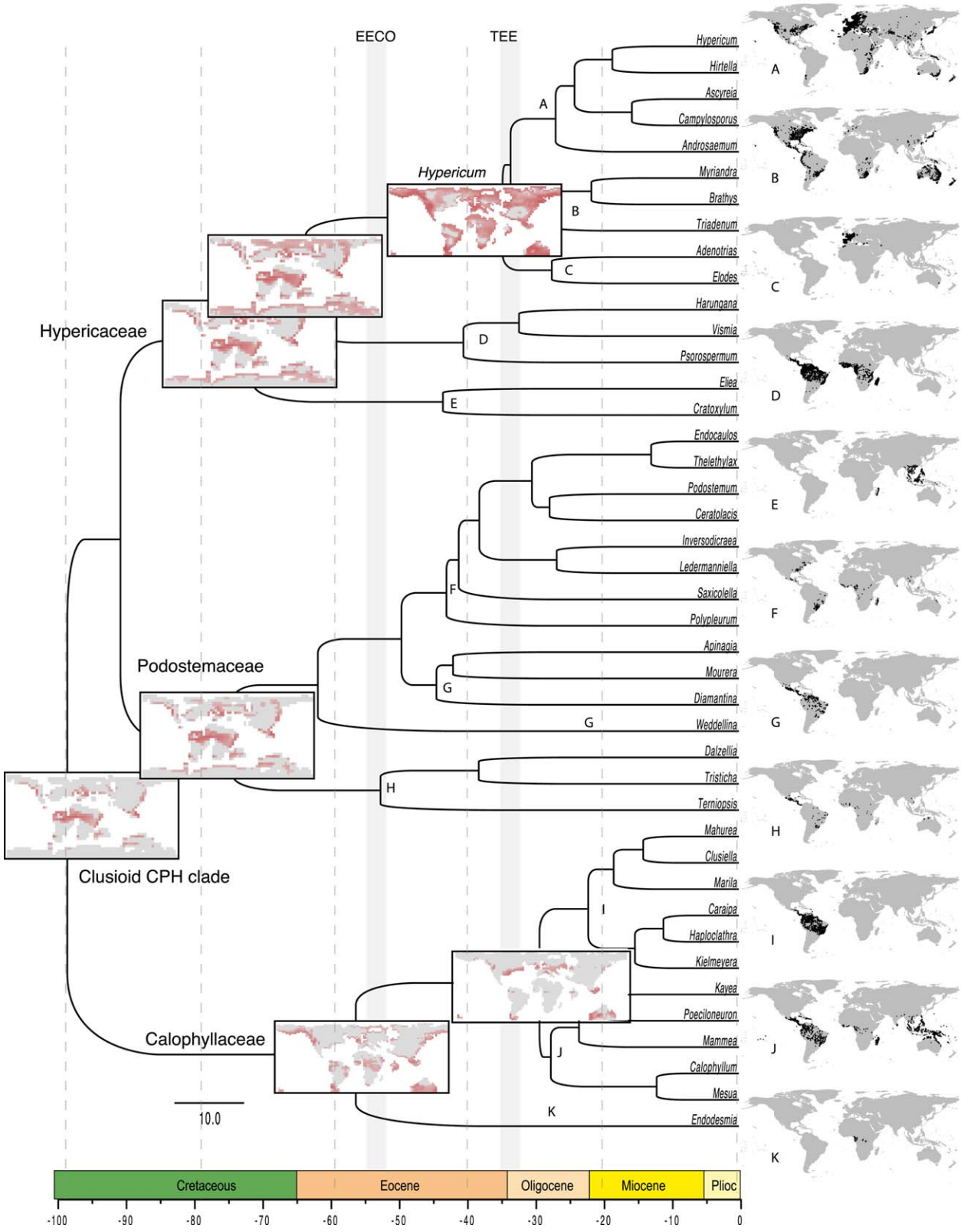

FIGURE 3 Potential distribution of the clusioid Calophyllaceae, Podostemaceae and Hypericaceae (CPH) clade in the past (in red) derived from the ancestral niche reconstruction calibrated with fossils. Estimated ancestral niche values are projected over a suite of palaeoclimate reconstructions and plotted over the clusioid CPH clade tree. Maps on the right represent occurrences used in this study and reflect present ranges of the taxa. Abbreviations: EECO = Early Eocene Climate Optimum; TEE = Terminal Eocene Event

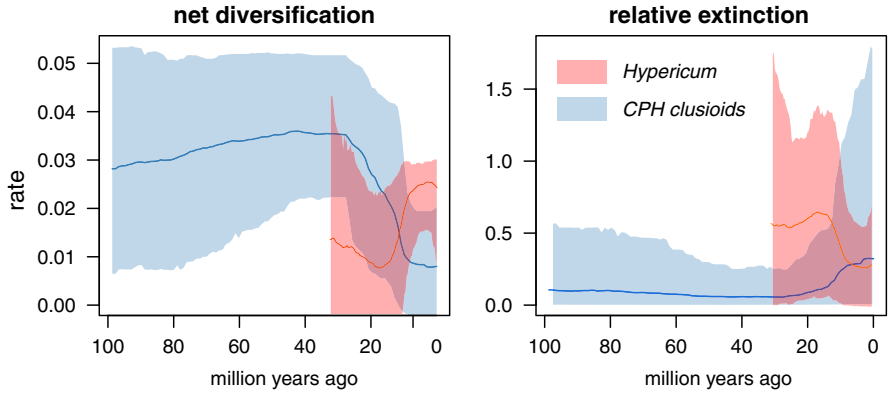

FIGURE 4 Net diversification (speciation-extinction) and relative extinction (extinction/speciation) of the clusioid Calophyllaceae, Podostemaceae and Hypericaceae (CPH) clade and *Hypericum* through time as estimated by the episodic model of TESS (CoMET)

as likely characterized by warm subtropical climates (Crepet & Nixon, 1998).

Today, each of the three clusioid CPH families, Calophyllaceae, Podostomeceae and Hypericaceae, exhibits an amphi-tropical distribution, with different genera inhabiting the Neotropics, Southeast Asia, and Africa (Figure 3). Ruhfel et al. (2016) argued the disjunct distribution across former Gondwanan landmasses was achieved by 'boreotropical migration' during the Early Cenozoic or long-distance dispersal, rather than by ancient vicariance. The 'boreotropical connection' hypothesis posits that current widespread tropical lineages were formerly present in the Northern Hemisphere when climates were warm and humid at the start of the Cenozoic, but became extinct in these regions and moved, or were restricted to equatorial regions as climates became cooler following the TEE (Davis et al., 2002; Lavin & Luckow, 1993; Morley, 2007). Our ancestral niche and diversification analyses support this hypothesis. Geographical projections of ancestral climatic preferences show that ancestors of the clusioid CPH lineages could have found favourable conditions in the Northern Hemisphere before Cenozoic climate cooling (Figure 3), which is in agreement with the fossil record (Cavagnetto & Anadón, 1996) and with biogeographical reconstructions supporting the presence of Hypericaceae ancestors (*c.* 71 Ma) in the Holarctic (Meseguer et al., 2015). Our continuous diversification models also indicate a trend of increasing extinction rates through time in the CPH clusioid clade, while the episodic model supports a scenario with a decline in diversification rates and increase in the extinction fraction towards the end of the Eocene (Figure 4). It is possible that, when paratropical conditions disappeared from the Holarctic (Morley, 2007), these clusioid lineages failed to adapt to new temperate regimes and went extinct, persisting in refugia in southern tropical regions (Figures 2 and 3). Similar scenarios of climate-driven extinction have been inferred in other angiosperms facing climate cooling (Antonelli & Sanmartín, 2011; Willis & MacDonald, 2011; Xing et al., 2014).

4.2 | Late Cenozoic evolution of *Hypericum*: temperate niche shifts, diversification, and geographical expansion into tropical mountains

Meseguer et al. (2015) suggested that *Hypericum* stem-lineages were distributed in the Holarctic before the EECO, and could have been part of the Early Cenozoic boreotropical flora. Our results support this hypothesis. Climatic preferences for the *Hypericum* stem-node were inferred to be more similar to those observed today among other tropical Hypericaceae taxa – and other CPH lineages – than to extant *Hypericum* species (Figure 2). Geographical projections of these climatic preferences show climatically suitable conditions for stem-*Hypericum* in the Holarctic during the Palaeocene (*c.* 64 Ma; Figure 3). By the TEE, concurrent with climate cooling (*c.* 35 Ma), the MRCA of all extant species (*Hypericum* crown-node) was already inferred to be adapted to temperate conditions: tolerating average temperatures up to −6 °C during the coldest month of the year, and drier environments than its ancestors, with less than 1000 mm of annual precipitation (Figure 2, Supporting Information Appendices S7–S10). This supports the idea that an event of climate niche evolution along the stem-branch of *Hypericum*, the acquisition of new temperate tolerances, allowed this genus to persist in the Holarctic after the TEE dramatic transition, whereas other clusioid relatives went extinct (Meseguer et al., 2013, 2015).

A previous study (Nürk et al., 2015) has also inferred a climatic niche shift towards temperate tolerances at the onset of *Hypericum* diversification, but this event is dated later during the Oligocene. The estimated Oligocene age for crown-*Hypericum* by Nürk et al. (25.8 Ma, 95% HPD = 33–20 Ma; cf. Figure 2) is about 10 Myr younger than the one estimated in Meseguer et al. (2015) – Late Eocene 34.9 Ma (HPD = 34–37 Ma, Supporting Information Figure S4.2). It also differs from the Ruhfel et al. (2016) analysis of the clusioid clade (37.3 Ma, HPD = 26–52 Ma, Supporting Information Figure S4.1), which employed a different set of fossils, and from a more comprehensive analysis of Malpighiales dating the crown group of the New World clade of *Hypericum* at 25 Ma (Xi et al., 2012), which is otherwise in agreement with our estimates for this node (29 Ma; HDP 23–33 Ma). Nürk et al.'s biogeographical reconstruction is also in conflict with the boreotropical hypothesis (stem lineages were reconstructed during the greenhouse period of the Eocene, including the EECO, in Africa) and in disagreement with the fossil record (Meseguer & Sanmartín, 2012; see further discussion in Supporting Information Appendix S3).

Were these temperate preferences conserved over evolutionary time in *Hypericum*? Overall, temperate preferences similar to those of

crown-node *Hypericum* are shared by subclades such as North American section *Myriandra* or semiaquatic Mediterranean *Elodes* (Figure 2). However, a trend towards increasing tolerance to cold can be observed in some lineages, such as the MRCA of *Hirtella*, with species widely distributed in Eurasia. Three *Hypericum* lineages were reconstructed in Meseguer et al. (2013) as migrating into the southern tropical mountains after the LMC event (*c*. 10 Ma): the *Campylosporus* s.l. clade in eastern Africa, *Brathys* in the Andean Paramo and *Ascyreia* in the Himalayas. Although the common view is that the Miocene–Pliocene uplift of these mountains opened new areas with similar climatic conditions for temperate taxa, which promoted rapid diversification in pre-adapted taxa (Graham et al., 2014; Merckx et al., 2015), our results suggest that *Hypericum* did not experience the same temperate conditions in these regions as in the Holarctic. Species of *Ascyreia* and *Brathys* occur in more humid environments than those inhabited by other extant *Hypericum* species (excepting in section *Hypericum* s.s.), and than those inferred for their *Hypericum*-crown ancestors (Figure 2). Their precipitation tolerances are indeed more similar to those of other tropical clusioid CPH lineages. Temperature tolerances for *Campylosporus* are also the most similar to the ones inferred for tropical stem-*Hypericum*. All of this suggests a remarkable ability of *Hypericum* to occupy different environments within the temperate biome, with climatic preferences being to a certain degree phylogenetically labile in this lineage (Evans, Smith, Flynn, & Donoghue, 2009; Wüest, Antonelli, Zimmermann, & Linder, 2015).

Was the shift to temperate tolerances key for the evolutionary success of *Hypericum*? A general tenet in evolutionary ecology is that the acquisition of new climatic preferences allows a lineage to colonize novel ecological niches (*e.g.* temperate habitats), which can promote rapid diversification by ecological release, that is, the availability of novel resources and reduction in direct competition (Wiens et al., 2010). We found no direct correlation between the event of niche evolution before crown-*Hypericum* ($>$ 35 Ma) and an increase in diversification rates in the genus. Instead, we found that extinction rates decreased and speciation rates increased in *Hypericum* after climates became increasingly colder with the Late Miocene climate cooling, *c*. 10 Ma (Figure 4). This increase in diversification in the Late Miocene coincides with Meseguer et al.'s (2013) reconstruction of migration events into the newly uplifted tropical mountains during this period within *Brathys* (Andes), *Ascyreia* (Himalayas) and *Campylosporus* (Africa), and with the inference of potential climatic adaptation in these clades (Figure 2).

4.3 | The boreotropical roots of temperate taxa

The TEE was probably the most dramatic climate cooling of the last 100 Myr, representing a vegetation turnover at a scale (temporal, geographical, compositional) not seen later (Morley, 2007), and has often been associated with historically high extinction rates in Holarctic plants (Antonelli & Sanmartín, 2011; Willis & MacDonald, 2011; Xing et al., 2014). Willis and MacDonald (2011) found that persistence and adaptation was the predominant response in the plant fossil record under Cenozoic climate warming. Here, we have found a mixed response of different clusioid lineages facing climate cooling, with evidence of extinction and/or migration when paratropical conditions disappeared from the Holarctic (ancestors of the CPH clusioid lineages), but also evidence of adaptation to more temperate, colder climates (*Hypericum* ancestors).

Interestingly, *Hypericum* might not be unique in its adaptive response. Based on the early Cenozoic fossil record, Wolfe (1977) argued that the climatic tolerances of characteristic modern temperate taxa, such as *Alnus*, *Quercus*, *Laurus*, *Fagus*, *Betula*, *Platanus*, *Carya*, *Ulmus* or *Vitis* in North America, or *Populus*, *Salix*, *Myrica*, *Carpinus*, *Rubus*, *Ilex*, *Acer* and *Tilia* in Eurasia, changed in the Holarctic concurrent with the TEE. Further studies are needed to understand whether these temperate genera descend from ancient (para)tropical taxa and, as *Hypericum*, evolved temperate tolerances *in situ*. To clarify this, a combination of palaeontological and neontological data is needed (Meseguer et al., 2015; Slater et al., 2012). This is because if climate change is rapid and intense, it can have a clade-wide effect, driving entire lineages to extinction or promoting niche evolution across all members of a clade (Eiserhardt, Borchsenius, Plum, Ordonez, & Svenning, 2015; Spriggs et al., 2015), in which case, evidence of ancestral climatic tolerances might be lost from extant taxa. Including fossil evidence in our ancestral niche reconstructions, here limited to crown-node *Hypericum*, did not change the inferred trend but contributed to decreasing uncertainty in the ASR inferences (Figure 2, Supporting Information Figure S4.3). Conversely, inclusion of fossil evidence might be critical to reconstructing the evolutionary fate of other lineages that were part of the now-vanished, ancient 'boreotropical' forest, such as the ancestors of the CPH clusioid clade, because extinction was inferred to be high in these clades.

5 | CONCLUSIONS

Overall, our reconstructions are consistent with hypotheses of a post K-Pg origin of modern tropical rain forests (Wing et al., 2009), with preferences for more humid environments evolving independently in the CPH clade families Calophyllaceae and Hypericaceae in the early Cenozoic ($<$ 60 Ma). We also find support for an ancient geographical distribution of paratropical taxa in northern latitudes concurrent with the Late Palaeocene–Eocene climate warming. Subsequent climate cooling triggered diversification declines in CPH tropical lineages, and their disappearance from northern latitudes. The main exception was *Hypericum*, for which TEE climate cooling triggered a climatic shift towards temperate affinities. This adaptation was probably crucial for the evolutionary success of *Hypericum*, the most species-rich and widespread of all clusioid genera. Yet, rather than initial rapid diversification by ecological release, the high diversity levels found today are explained by a combination of (a) geographical range expansions facilitated by plate tectonics and further (LMC) climate cooling enabling dispersal over tropical regions; and (b) Neogene niche evolution into temperate wetter habitats along tropical mountains in clades such as *Brathys* and *Ascyreia*.

ACKNOWLEDGMENTS

Research funding was provided by the Spanish government through a PhD grant (AP-2007-01698) to ASM, and projects CGL2009–13322-C01, CGL2012–40129-C01 and CGL2015–67849-P (MINECO/FEDER) to IS. ASM was also supported by a Marie-Curie FP7–COFUND (AgreenSkills fellowship–26719) grant. This work benefited from an '*Investissements d'Avenir*' grant managed by Agence Nationale de la Recherche (CEBA, ref. ANR-10-LABX-25-01). JC is supported by Marie-Curie Actions People H2020, MSCA-IF-EF-ST-708207. The authors are grateful to Daniel Silvestro and all the anonymous referees who contributed to improving this work and to Martin Godefroid, Graham Slater and Sebastian Höhna for help with the analyses.

AUTHOR CONTRIBUTIONS

ASM, JML and IS designed the study; DB provided palaeoclimate data, and BRR and CCD the clusioid chronograms; ASM, JML, JC, and IS analysed the data; ASM and IS wrote the manuscript with contributions from JML, JC and EJ, and comments from all other authors.

DATA ACCESSIBILITY

All data used in this manuscript are presented in the manuscript and its supplementary material or have been previously published or archived elsewhere.

ORCID

Andrea S. Meseguer http://orcid.org/0000-0003-0743-404X

REFERENCES

Antonelli, A., & Sanmartín, I. (2011). Mass extinction, gradual cooling, or rapid radiation? Reconstructing the spatiotemporal evolution of the ancient angiosperm genus *Hedyosmum* (Chloranthaceae) using empirical and simulated approaches. *Systematic Biology*, *60*(5), 596–615.

Beerling, D., Berner, R. A., Mackenzie, F. T., Harfoot, M. B., & Pyle, J. A. (2009). Methane and the CH4 related greenhouse effect over the past 400 million years. *American Journal of Science*, *309*, 97–113.

Beerling, D. J., Fox, A., Stevenson, D. S., & Valdes, P. J. (2011). Enhanced chemistry-climate feedbacks in past greenhouse worlds. *Proceedings of the National Academy of Sciences USA*, *108*, 9770–9775.

Betancur-R, R., Ortí, G., & Pyron, R. A. (2015). Fossil-based comparative analyses reveal ancient marine ancestry erased by extinction in ray-finned fishes. *Ecology Letters*, *18*, 441–450.

Boyce, C. K., Lee, J.-E., Field, T. S., Brodribb, T. J., & Zwieniecki, M. A. (2010). Angiosperms helped put the rain in the rainforests: The impact of plant physiological evolution on tropical biodiversity. *Annals of the Missouri Botanical Garden*, *97*, 527–540.

Cavagnetto, C., & Anadón, P. (1996). Preliminary palynological data on floristic and climatic changes during the Middle Eocene-Early Oligocene of the eastern Ebro Basin, northeast Spain. *Review of Palaeobotany and Palynology*, *92*(3–4), 281–305.

Couvreur, T. L., Pirie, M. D., Chatrou, L. W., Saunders, R. M., Su, Y. C., Richardson, J. E., & Erkens, R. H. (2011). Early evolutionary history of the flowering plant family Annonaceae: Steady diversification and boreotropical geodispersal. *Journal of Biogeography*, *38*, 664–680.

Crepet, W. L., & Nixon, K. C. (1998). Fossil Clusiaceae from the late Cretaceous (Turonian) of New Jersey and implications regarding the history of bee pollination. *American Journal of Botany*, *85*(8), 1122–1133.

Davis, C. C., Bell, C. D., Mathews, S., & Donoghue, M. J. (2002). Laurasian migration explains Gondwanan disjunctions: Evidence from Malpighiaceae. *Proceedings of the National Academy of Sciences USA*, *99*, 6833–6837.

Davis, C. C., Webb, C. O., Wurdack, K. J., Jaramillo, C. A., & Donoghue, M. J. (2005). Explosive radiation of Malpighiales supports a mid-Cretaceous origin of modern tropical rain forests. *The American Naturalist*, *165*, E36–E65.

Dawson, T. P., Jackson, S. T., House, J. I., Prentice, I. C., & Mace, G. M. (2011). Beyond predictions: Biodiversity conservation in a changing climate. *Science*, *332*, 53.

Donoghue, M. J., & Edwards, E. J. (2014). Biome shifts and niche evolution in plants. *Annual Review of Ecology, Evolution, and Systematics*, *45*, 547–542.

Dormann, C. F., Elith, J., Bacher, S., Buchmann, C., Carl, G., Carré, G., … Lautenbach, S. (2013). Collinearity: A review of methods to deal with it and a simulation study evaluating their performance. *Ecography*, *36*(1), 27–46.

Eiserhardt, W. L., Borchsenius, F., Plum, C. M., Ordonez, A., & Svenning, J.-C. (2015). Climate-driven extinctions shape the phylogenetic structure of temperate tree floras. *Ecology Letters*, *18*, 263–272.

Evans, M. E. K., Smith, S. A., Flynn, R. S., & Donoghue, M. J. (2009). Climate, niche evolution, and diversification of the "bird-cage" evening primroses (*Oenothera*, sections *Anogra* and *Kleinia*). *The American Naturalist*, *173*, 225–240.

Gelman, A., & Rubin, D. B. (1992). Inference from iterative simulation using multiple sequences. *Statistical Science*, *7*(4), 457–511.

Graham, C. H., Carnaval, A. C., Cadena, C. D., Zamudio, K. R., Roberts, T. E., Parra, J. L., … Sanders, N. J. (2014). The origin and maintenance of montane diversity: Integrating evolutionary and ecological processes. *Ecography*, *37*(8), 711–719.

Hewitt, G. (2000). The genetic legacy of the quaternary ice ages. *Nature*, *405*(6789), 907–913.

Hijmans, R. J., Cameron, S. E., Parra, J. L., Jones, P. G., & Jarvis, A. (2005). Very high resolution interpolated climate surfaces for global land areas. *International Journal of Climatology*, *25*(15), 1965–1978.

Ho, L. S. T., & Ané, C. (2014). Intrinsic inference difficulties for trait evolution with Ornstein-Uhlenbeck models. *Methods in Ecology and Evolution*, *5*, 1133–1146.

Höhna, S., Landis, M. J., Heath, T. A., Boussau, B., Lartillot, N., Moore, B. R., … Ronquist, F. (2016). RevBayes: Bayesian phylogenetic inference using graphical models and an interactive model-specification language. *Systematic Biology*, *65*(4), 726–736.

Höhna, S., May, M. R., & Moore, B. R. (2016). TESS: An R package for efficiently simulating phylogenetic trees and performing Bayesian inference of lineage diversification rates. *Bioinformatics*, *32*(5), 789–791.

Huber, B. T., Norris, R. D., & MacLeod, K. G. (2002). Deep-sea paleotemperature record of extreme warmth during the Cretaceous. *Geology*, *30*(2), 123–126.

Jaramillo, C., Hoorn, M. C., Silva, S., Leite, F., Herrera, F., Quiroz, L., … Antonioli, L. (2010). The origin of the modern Amazon rainforest: Implications from the palynological and paleobotanical record. In M. C. Hoorn and F. P. Wesselingh (Eds.), *Amazonia, landscape and species evolution* (pp. 317–334). Oxford: Blackwell.

Johnson, K. R., & Ellis, B. (2002). A tropical rainforest in Colorado 1.4 Million years after the Cretaceous-Tertiary boundary. *Science*, *296*(5577), 2379–2383.

Lavin, M., & Luckow, M. (1993). Origins and relationships of tropical North America in the context of the boreotropics hypothesis. *American Journal of Botany*, *80*, 1–14.

May, M. R., Höhna, S., & Moore, B. R. (2016). A Bayesian approach for detecting the impact of mass-extinction events on molecular phylogenies when rates of lineage diversification may vary. *Methods in Ecology and Evolution*, *7*(8), 947–959.

Merckx, V. S. F. T., Hendriks, K. P., Beentjes, K. K., Mennes, C. B., Becking, L. E., Peijnenburg, K. T. C. A., … Schilthuizen, M. (2015). Evolution of endemism on a young tropical mountain. *Nature*, *524*, 347–350.

Meseguer, A. S., Aldasoro, J. J., & Sanmartin, I. (2013). Bayesian inference of phylogeny, morphology and range evolution reveals a complex evolutionary history in St. John's wort (*Hypericum*). *Molecular Phylogenetics and Evolution*, *67*, 379–403.

Meseguer, A. S., Lobo, J. M., Ree, R. H., Beerling, D. J., & Sanmartin, I. (2015). Integrating fossils, phylogenies, and niche models into biogeography to reveal ancient evolutionary history: The case of *Hypericum* (Hypericaceae). *Systematic Biology*, *64*(2), 215–232.

Meseguer, A. S., & Sanmartín, I. (2012). Paleobiology of the genus *Hypericum* (Hypericaceae): A survey of the fossil record and its palaeogeographic implications. *Anales del Jardín Botánico de Madrid*, *69*, 97–106.

Meyer, H. W., & Manchester, S. R. (1997). *The Oligocene Bridge Creek flora of the John Day formation, Oregon*. *Geological science*, Vol. *141*. 1–195.

Morley, R. J. (2000). *Origin and evolution of tropical rain forests*. New York: Wiley.

Morley, R. J. (2007). Cretaceous and Tertiary climate change and the past distribution of megathermal rainforests. In M. B. Bush & J.-R. Flenley (Eds.), *Tropical rainforest responses to climatic change* (pp. 1–31). Berlin, Germany: Springer.

Nürk, N. M., Uribe-Convers, S., Gehrke, B., Tank, D. C., & Blattner, F. R. (2015). Oligocene niche shift, Miocene diversification- cold tolerance and accelerated speciation rates in the St. John's Worts (*Hypericum*, Hypericaceae). *BMC Evolutionary Biology*, *15*, 80–93.

O'Meara, B. C. (2012). Evolutionary inferences from phylogenies: A review of methods. *Annual Review of Ecology, Evolution, and Systematics*, *43*, 267–285.

Otto-Bliesner, B. L., Marshall, S. J., Overpeck, J. T., Miller, G. H., & Hu, A. (2006). Simulating Arctic climate warmth and icefield retreat in the last interglaciation. *Science*, *311*, 1751.

Paradis, E., Claude, J., & Strimmer, K. (2004). APE: Analyses of phylogenetics and evolution in R language. *Bioinformatics*, *20*(2), 289–290.

Plummer, M., Best, N., Cowles, K., & Vines, K. (2006). CODA: Convergence diagnosis and output analysis for MCMC. *R News*, *1*, 7–11.

Pokorny, L., Riina, R., Mairal, M., Meseguer, A. S., Culshaw, V., Cendoya, J., … Sanmartin, I. (2015). Living on the edge: Timing of Rand flora disjunctions congruent with ongoing aridification in Africa. *Frontiers in Genetics*, *6*,

Robson, N. K. B. (2012). Studies in the genus *Hypericum* L. (Hypericaceae) 9. Addenda, corrigenda, keys, lists and general discussion. *Phytotaxa*, *72*, 1–111.

Ruhfel, B. R., Bittrich, V., Bove, C. P., Gustafsson, M. H. G., Philbrick, C. T., Rutishauser, R., … Davis, C. C. (2011). Phylogeny of the clusioid clade (Malpighiales): Evidence from the plastid and mitochondrial genomes. *American Journal of Botany*, *98*, 306–325.

Ruhfel, B. R., Bove, C. P., Philbrick, C. T., & Davis, C. C. (2016). Dispersal largely explains the Gondwanan distribution of the ancient tropical clusioid plant clade. *American Journal of Botany*, *103*, 1117–1128.

Ruhfel, B. R., Stevens, P. F., & Davis, C. C. (2013). Combined morphological and molecular phylogeny of the clusioid clade (Malpighiales) and the placement of the ancient rosid macrofossil *Paleoclusia*. *International Journal of Plant Sciences*, *174*, 910–936.

Slater, G. J., Harmon, L. J., & Alfaro, M. E. (2012). Integrating fossils with molecular phylogenies improves inference of trait evolution. *Evolution*, *66*, 3931–3944.

Spriggs, E. L., Clement, W. L., Sweeney, P. W., Madriñan, S., Edwards, E. J., & Donoghue, M. J. (2015). Temperate radiations and dying embers of a tropical past: The diversification of *Viburnum*. *New Phytologist*, *207*, 1469–8137.

Stevens, P. F. (2007). Clusiaceae-Guttiferae. In K. Kubitzki (Ed.), *The families and genera of vascular plants* (pp. 48–66). Berlin: Springer.

Svenning, J.-C., Eiserhardt, W. L., Normand, S., Ordonez, A., & Sandel, B. (2015). The influence of paleoclimate on present-day patterns in biodiversity and ecosystems. *Annual Review of Ecology, Evolution, and Systematics*, *46*, 551–572.

Tiffney, B. H. (1985). Perspectives on the origin of the floristic similarity between eastern Asia and eastern North America. *Journal of the Arnold Arboretum*, *66*, 73–94.

Töpel, M., Zizka, A., Calió, M. F., Scharn, R., Silvestro, D., & Antonelli, A. (2017). SpeciesGeoCoder: Fast categorization of species occurrences for analyses of biodiversity, biogeography, ecology, and evolution. *Systematic Biology*, *66*, 145–151.

Upchurch, G. R., & Wolfe, J. A. (1987). Mid-Cretaceous to early tertiary vegetation and climate: Evidence from fossil leaves and woods. In E. M. Friis, W. G. Chaloner, & J. C. Crane (Eds.), *The origins of Angiosperms and their biological consequences* (pp. 75–105). UK: Cambridge University Press.

Wiens, J. J., Ackerly, D. D., Allen, A. P., Anacker, B. L., Buckley, L. B., Cornell, H. V., … Stephens, P. R. (2010). Niche conservatism as an emerging principle in ecology and conservation biology. *Ecology Letters*, *13*, 1310–1324.

Wilf, P., Johnson, K. R., & Huber, B. T. (2003). Correlated terrestrial and marine evidence for global climate changes before mass extinction at the Cretaceous–Paleogene boundary. *Proceedings of the National Academy of Sciences USA*, *100*, 599–604.

Willis, K. J., & MacDonald, G. M. (2011). Long-term ecological records and their relevance to climate change predictions for a warmer world. *Annual Review of Ecology, Evolution, and Systematics*, *42*, 267–287.

Wing, S. L., Herrera, F., Jaramillo, C. A., Gómez-Navarro, C., Wilf, P., & Labandeira, C. C. (2009). Late Paleocene fossils from the Cerrejón Formation, Colombia, are the earliest record of Neotropical rainforest. *Proceedings of the National Academy of Sciences USA*, *106*(44), 18627–18632.

Wing, S. L., Strömberg, C. A. E., Hickey, L. J., Tiver, F., Willis, B., Burnham, R. J., & Behrensmeyer, A. K. (2012). Floral and environmental gradients on a Late Cretaceous landscape. *Ecological Monographs*, *82*, 23–47.

Wolfe, J. A. (1975). Some aspects of plant geography of the Northern Hemisphere during the Late Cretaceous and Tertiary. *Annals of the Missouri Botanical Garden*, *62*(2), 264–279.

Wolfe, J. A. (1977). Paleogene floras from the Gulf of Alaska region. *U.S. Geological Survey*, *997*, 1–108.

Wolfe, J. A. (1992). Climatic, floristic, and vegetational changes near the Eocene/Oligocene boundary in North America. In D. R. Prothero and W. A. Berggren (Eds.), *Eocene-Oligocene climatic and biotic evolution: Princeton Series in Geology and Paleontology* (pp. 421–436). NJ: Princeton University Press.

Wolfe, J. A., & Upchurch, G. R. (1987). North American nonmarine climates and vegetation during the Late Cretaceous. *Palaeogeography, Palaeoclimatology, Palaeoecology*, *61*, 33–77.

Wüest, R. O., Antonelli, A., Zimmermann, N. E., & Linder, H. P. (2015). Available climate regimes drive niche diversification during range expansion. *The American Naturalist*, *185*, 640–652.

Wurdack, K. J., & Davis, C. C. (2009). Malpighiales phylogenetics: Gaining ground on one of the most recalcitrant clades in the angiosperm tree of life. *American Journal of Botany*, *96*(8), 1551–1570.

Xi, Z., Ruhfel, B. R., Schaefer, H., Amorim, A. M., Sugumaran, M., Wurdack, K. J., ... Davis, C. C. (2012). Phylogenomics and a posteriori data partitioning resolve the Cretaceous angiosperm radiation Malpighiales. *Proceedings of the National Academy of Sciences USA*, *109*, 17519–17524.

Xing, Y., Onstein, R. E., Carter, R. J., Stadler, T., & Linder, P. H. (2014). Fossils and a large molecular phylogeny show that the evolution of species richness, generic diversity, and turnover rates are disconnected. *Evolution*, *68*, 2821–2832.

Zachos, J. C., Dickens, G. R., & Zeebe, R. E. (2008). An early Cenozoic perspective on greenhouse warming and carbon-cycle dynamics. *Nature*, *451*, 279–283.

Zanne, A. E., Tank, D. C., Cornwell, W. K., Eastman, J. M., Smith, S. A., FitzJohn, R. G., ... Beaulieu, J. M. (2014). Three keys to the radiation of angiosperms into freezing environments. *Nature*, *506*, 89–92.

Ziegler, A., Eshel, G., Rees, P. M., Rothfus, T., Rowley, D., & Sunderlin, D. (2003). Tracing the tropics across land and sea: Permian to present. *Lethaia*, *36*, 227–254.

BIOSKETCHES

Andrea S. Meseguer is a postdoctoral researcher at ISEM (CNRS, France) interested in macroevolution, in the factors and processes generating geographical and diversity patterns.

Isabel Sanmartín is a senior researcher at the Real Jardín Botánico (CSIC, Spain). Her main research interests include the study of large-scale biogeographical patterns, and the development of parametric methods in biogeography and macroevolution.

SUPPORTING INFORMATION

Additional Supporting Information may be found online in the supporting information tab for this article.

How to cite this article: Meseguer AS, Lobo JM, Cornuault J, et al. Reconstructing deep-time palaeoclimate legacies in the clusioid Malpighiales unveils their role in the evolution and extinction of the boreotropical flora. *Global Ecol Biogeogr*. 2018;27:616–628. https://doi.org/10.1111/geb.12724

Appendix S2. List of fossil seed occurrences used in the study modified from Meseguer et al. (2015). Abbreviations: Lat.= Latitude, Long. = Longitud, RotLat = rotated latitude, RotLong = rotated longitude. RotLat and RotLong refer to the latitude and longitude coordinates of the geographic location in the past, as it differs from the present coordinates given the rotation of the tectonics plates on the globe. Fossil paleocoordinates were calculated with the PointTracker application of the Paleomap software (Scotese 2010).

Epochs	subperiod	Fossil species	Lat.	Long.	RotLat	RotLong	Location	Reference
Eocene	Late	*Hypericum antiquum* Balueva et Nikit..	54.67	81.03	53.86	72.85	Uzhanikha, Novosibirskaya oblast, Russia	Arbuzova, 2005
Oligocene	Early	*Hypericum sp.*	41.48	1.33	37.13	-0.42	Catalonia, Spain	Cavagnetto & Anadón 1995
Oligocene	Early	*Hypericum septestum* Nikitin	56.48	84.97	55.93	76.29	Tomsk, Lagernyi Sad, Russia	Arbuzova, 2005
Oligocene	Late	*Hypericum miocenicum* Dorof. emend. Mai	51.05	15.00	46.97	11.31	Sachsen, Germany	Mai, 1997
Oligocene	Late	*Hypericum septestum* Nikitin	51.05	15.00	46.97	11.31	Sachsen, Germany	Mai, 1997
Oligocene	Late	*Hypericum septestum* Nikitin	51.07	14.10	46.98	10.48	Sachsen, Germany	Mai, 1997
Oligocene	Late	*Hypericum septestum* Nikitin	59.02	81.00	58.17	71.80	Tomsk, Russia	Dorofeev, 1963
Oligocene	Late	*Hypericum septestum* Nikitin	59.02	81.00	58.17	71.80	Tomsk, Russia	Dorofeev, 1963
Oligocene	Late	*Hypericum septestum* Nikitin	59.02	81.00	58.17	71.80	Tomsk, Russia	Dorofeev, 1963
Oligocene	Late	*Hypericum septestum* Nikitin	56.08	82.08	55.33	73.56	Tomsk, Russia	Dorofeev, 1963
Oligocene	Late	*Hypericum septestum* Nikitin	51.43	15.08	47.35	11.37	Gozdnica, Poland	Zastawniak et al., 1992
Oligocene		*Hypericum bornense* Mai	51.02	12.08	46.89	8.63	Sachsen, Germany	Mai & Walther, 1978
Oligocene		*Hypericum septestum* Nikitin	57.00	83.08	56.31	74.32	Tomsk, Russia	Dorofeev, 1963
Oligocene		*Hypericum septestum* Nikitin	57.00	83.08	56.31	74.32	Tomsk, Russia	Dorofeev, 1963

Appendix S3

Expanded Material and Methods

Rationale for the use of fossils and molecular age estimation analyses

Hypericum: For *Hypericum*, we used the phylogeny published by Meseguer & colleagues (Meseguer, Aldasoro & Sanmartin, 2013). This includes DNA sequences of three chloroplast markers (*psbA-trnH, trnL-trnF* and *trnS-trnG*) for 114 *Hypericum* specimens. Meseguer et al. (2013) analyzed different concatenated plastid datasets varying in the amount of missing data to evaluate the effect on phylogenetic reconstruction. Of these, we selected the matrix called "Two-markers" that only includes those specimens represented in at least two of the chloroplast markers (N=114). The reduction in missing data allowed recovering a tree with higher resolution and branch support values than the complete dataset including all specimens ("All-specimens", N=192), while at the same time recovering most of the morphological (92% of traditionally described sections) and all geographical variation within the genus (Robson, 2012). The phylogeny includes representatives of genera *Triadenum* and *Thornea,* which have been included within *Hypericum* in previous phylogenetic analyses (Ruhfel, Bittrich, Bove, Gustafsson, Philbrick et al., 2011; Meseguer et al., 2013; Nürk, Madriñán, Carine, Chase & Blattner, 2013), as well representatives of Hypericaceae genera *Eliea* (tribe Cratoxyleae) and *Vismia, Harungana* and *Psorospermum* (tribe Vismieae). Absolute ages were calculated using Bayesian relaxed molecular clock methods in BEAST v.1.8.1 (Drummond, Suchard, Xie & Rambaut, 2012) and the Late Eocene fossil *Hypericum antiquum* (Arbuzova, 2005) to calibrate the crown node of *Hypericum* (Meseguer, Lobo, Ree, Beerling & Sanmartin, 2015). Meseguer et al. (2015) provided a detailed explanation on the reliability of the *Hypericum* fossil record, and the assignment of fossils to specific clades in the phylogeny, based on a morphological study of the *Hypericum* fossil record (Meseguer & Sanmartín, 2012). Here, we reproduce this text to justify our choice of calibration settings (page 218, cf. Meseguer et al., 2015): "The oldest fossil remains of the genus, the Late Eocene fossil seeds of *H. antiquum*, have been found in West Siberia (Arbuzova, 2005). These fossil seeds share with genus *Hypericum* characteristics like their small size (0.4-0.65 x 0.25-0.35mm), black color, and cylindrical shape (*i.e.* seeds are longitudinally slightly bent towards the raphe). Moreover, the presence of meridian ribs on the fossil seed testa resemble the "ribbed scalariform" pattern present in various extant sections that are grouped into three distantly related clades in Meseguer et al. (2013)'s phylogeny: the early diverging section *Elodes* (clade A), the New World sister-sections *Brathys* and *Trigynobrathys* (clade B), and the Old

World section *Drosocarpium* (clade E). No additional characters in the seeds of these sections, though, allow us to assign the fossil to one of them (Meseguer & Sanmartín, 2012). Magallón and Sanderson (page 1766) suggested that in the absence of explicit phylogenetic analyses including the fossil, the existence of synapomorphies could be used as an empirical criterion to determine the phylogenetic assignment of fossils. If a fossil presents the synapomorphies that characterize the extant members of a particular subclade within a larger clade, then this fossil can be assigned unambiguously to the crown group of the larger clade (e.g., *H. antiquum* displays the ribbed scaraliform sculpture pattern characteristic of the *Elodes* subclade whithin *Hypericum,* so it can be identified as a crown group member of genus *Hypericum*). Conversely, if a fossil displays some, but not all the synapomorphies shared by extant members of a clade, then it is considered to be a stem lineage representative. Besides the scalariform seed testa, the fossil seeds of *H. antiquum* do not display any other particular feature (apomorphy) that distinguishes them from the seeds of other extant clades in *Hypericum*. Therefore, in here we chose to follow a conservative approach (Magallón & Sanderson, 2001; Ho & Phillips, 2009) and assign the fossil remains of *Hypericum antiquum* to the crown node from which all living *Hypericum* are descendants, which is also the most recent common ancestor of the three clades exhibiting the scalariform seed testa, *i.e.* clades A, B, and E (Meseguer et al., 2013). The next oldest fossil remains are seeds of the fossil species *H. septestum,* from Lower Oligocene deposits again in the Eastern Palearctic region (Tomsk, Russia) (Arbuzova, 2005). This species became a common element in the Palearctic fossil record of the genus from the Late Oligocene to the Pliocene (Meseguer & Sanmartín, 2012). Although characters such as the size, color and disposition of the appendages identify these seeds as belonging to *Hypericum* (see above), the sculpturing pattern of the testa (*i.e.* reticulate) is the most common within *Hypericum* and it is also present in other genera. Thus, these fossil seeds could not be assigned with confidence to any subclade within *Hypericum* based on this character, and we did not use them for node calibration in any subsequent dating or biogeographic analyses. The same applied to other Oligocene to Pleistocene fossils such as *H. tertiarium* Nikitin, *H. miocenicum* Dorof. emend. Mai or *H. holyi* Friis, and to other remains that have been attributed to extant species of *Hypericum*, such as *Hypericum perforatum fossilis* or *H. androsaemum fossilis* (Meseguer & Sanmartín, 2012), which have also reticulate testa patterns".

Based on these fossil calibrations, Meseguer et al. (2015) obtained a crown age of Hypericaceae of 53.8 Ma with a very broad confidence interval (95% HPD = 43 – 66 Ma; **Fig. S2**). Divergence between tribes Hypericeae (=*Hypericum*) and Vismieae occurred during the Early

Eocene (49.9 Ma; 95% HPD = 41 – 60 Ma), while crown-group *Hypericum* is dated as Late Eocene, 34.9 Ma (95% HPD = 34 – 37 Ma). Divergence between the New World and Old World groups is dated in the Eocene–Oligocene boundary (33.7 Ma; 95% HPD = 30 – 37 Ma), whereas divergence within the three major clades A–C defined by Meseguer et al. (2013) is dated as Early Oligocene (**Fig. S2**).

Recently, Nürk et al. (2015) also estimated ages of divergence within genus *Hypericum*; their estimated age for crown-group *Hypericum* (25.8 Ma, 95% HPD = 33–20 Ma; cf. Fig. 2) is about 10 Ma younger than ours and differ also from more inclusive analyses on the clusioid clade, using different set of fossils (37.3 Ma, HPD = 26–52 (Ruhfel, Bove, Philbrick & Davis, 2016)). In their comprehensive dating analysis of Malpighiales, Xi et al., (2012) dated the crown group of the New World clade of *Hypericum* at 25 Ma, which is in agreement with our estimates for this node (29 Ma; HDP 23–33) (Xi, Ruhfel, Schaefer, Amorim, Sugumaran et al., 2012). The age discrepancy with Nürk's study can be explained by a different assignment of the fossil *H. antiquum*, which was used to calibrate the stem-node of the genus. As discussed above, these fossil seeds do not possess any distinguishable character that differs from extant *Hypericum* taxa, while they share a synapomorphy (a ribbed-scalariform seed testa) with unrelated *Hypericum* clades *Elodes, Brathys, Trigynobrathys and Drosocarpium*, whose *mrca* is also the crown node of the genus (Meseguer & Sanmartín, 2012). Therefore, the most conservative approach would be to place this fossil at the crown node of the genus (Magallón & Sanderson, 2001; Ho & Phillips, 2009). In addition, Nürk et al. (2015) used some more recent fossils to calibrate internal nodes in their phylogeny: seeds of *Hypericum tertiaerum* Nikitin from the Miocene, *H. virginicum* from the Pleistocene and Pliocene seeds assigned to *H. perforatum,* as well as *Hypericum* pollen and a macrofossil leaf assigned to *H. xylosteifolium* from the Upper Pliocene. Although the seeds probably belong to *Hypericum* (see above), they lack diagnostic characters (synapomorphies) to be assigned with confidence to any clade within the genus (Meseguer & Sanmartín, 2012; Meseguer et al., 2013).

In a recent study on the biogeography of the clusioid clade, Ruhfel and collaborators (Ruhfel et al., 2016) stated that they did not use the Eocene fossils seeds of *Hypericum antiquum* as an age constraint in their tree because this fossil shares similarities with *Elatine* (Elatinaceae), *Nymphaea* (Nymphaeaceae), and Passifloraceae *s.l.* (Stevens, 2001 onward). We disagree with this statement. *Nymphaea* seeds are generally larger than 1 mm, the shape is globose-circular to ovate, the colour green to light brown, and they do not present ribbed scalariform testas; the testa of *Nymphaea* seeds often presents characteristic trichomes arranged in rows (Bonilla-

Barbosa, Novelo, Hornelas Orozco & Márquez-Guzmán, 2000). Conversely, *Hypericum* species from sections *Elodes*, *Drossocarpium* or *Brathys* possess ribbed-scalariform testas, brown to black in colour, and with characteristic oblong to elliptic shapes (Robson, 1981); the same synapomorphies are present in the fossil seeds of *Hypericum antiquum* (Meseguer & Sanmartín, 2012). On the other hand, Passifloraceae seeds are characterized by a larger size, usually larger than (3)4 mm, the presence of an apiculum and an aril, and the testas are reticulated, pitted to striate, and ovate to obovate in shape (Alvarado-Cárdenas, 2007). Some *Elatinae* seeds are within the size range described for *Hypericum* but they do not display ribbed-scalariform testas; instead, the ornamentation is foveo-reticulate and seeds tend to be slightly to strongly- bent (e.g. (Molnár V, Horváth, Tökölyi & Somlyay, 2013; Popiela, Łysko, Molnár V, Kącki & Lukács, 2015).

Clusioid clade: For the clusioid clade, we used the clusioid chronogram of (Ruhfel et al., 2016), which was dated in BEAST v.1.8.1 (Drummond et al., 2012) using Bayesian relaxed molecular clock methods. The original dataset included several plastid (*matK, ndhF,* and *rbcL*) and mitochondrial (*matR*) markers and represented 52 of the 94 currently recognized clusioid genera (Ruhfel et al., 2016) (**Fig. S1**). For estimating absolute ages in the clusioid clade, the authors used the Eocene fossil *Pachydermites diederexii* to constrain the age of crown Symphonieae, and the Turonian (Late Cretaceous) fossil *Palaeoclusia chevalieri* (Crepet & Nixon, 1998). In a previous dating of the clusioid phylogeny, (Ruhfel, 2011) explored two different positions for *Paleoclusia*: as the stem age of the clusioid clade (the MRCA of Ochnaceae *s.l.* and the clusioid clade, "OC position"), and as the stem node of the Clusiaceae family (the MRCA of Bonnetiaceae and Clusiaceae *s.s.,* "BC position"). However, a recent study based on a combined DNA and morphological matrix for extant and fossil species, suggested that *Paleoclusia* was probably a stem (BC position) or a crown relative of Clusiaceae *s.s.* (Ruhfel, Stevens & Davis, 2013). To account for this evidence on the phylogenetic placement of *Palaeoclusia*, they also used this fossil to constrain the crown age of Clusiaceae s.s. (CC position). The root node was set to a uniform distribution between 89.3 and 125 Ma. The former age corresponds to the minimum age of the oldest known fossil within Malpighiales (*Paleoclusia*), while the later date corresponds to the earliest evidence of tricolpate pollen (Magallón, Crane & Herendeen, 1999; Sanderson & Doyle, 2001). Tricolpate pollen is a synapomorphy of the eudicot clade to which Malpighiales belong (APG III, 2009). Results of the dating analysis of the clusioid clade under the BC position of *Paleoclusia* appear in **Fig. S1** on Appendix S4 and were used for further analyses in this study, since this datation is the one that is more congruent with the *Hypericum* datation of

Meseguer et al. (2015), using a different set of fossils. For the CC placement, the crown age of the clusioid clade was estimated at 112 Ma with a small confidence interval (CI=105–116 Ma). The crown origin of the major families of Malpighiales ranges from the Late Cretaceous to the Early Cenozoic: 58 Ma (CI=38–87 Ma) for Bonnetiaceae; 91 Ma (CI=89–92 Ma) for Clusiaceae s.s.; 54 Ma (CI=27–76 Ma) for Calophyllaceae; 80 Ma (CI=73–87 Ma) Podostemaceae and 77 Ma (CI=64–93 Ma) for Hypericaceae. Divergence times calculated by Ruhfel (Ruhfel, 2011) for the clusioid BC phylogeny are slightly younger but overall in agreement with the CC dates (**Fig. S1**); the crown age of the clusioid clade was estimated at 103 Ma. The crown origin of the major families is 52 Ma (CI=31–76 Ma) for Bonnetiaceae; 63 Ma (CI=52–76 Ma) for Clusiaceae *s.s.*; 56 Ma (CI=30–84 Ma) for Calophyllaceae; 75 Ma (CI=64–87 Ma) Podostemaceae and 71 Ma (CI=56–86 Ma) for Hypericaceae. Differences between the CC and BC placements of *Paleoclusia* mostly affect the stem-age of Clusiaceae s.s, which is considerably older in the CC tree.

REFERENCES

Alvarado-Cárdenas, L.O. (2007) Flora del Valle de Tehuacán-Cuicatlán. Passifloraceae. (ed. by M. Lemos). Departamento de Botánica, Instituto de Biología, UNAM, Mexico.

Arbuzova, O. (2005) *Hypericum* L. *Iskopaemye tsvetkovye rastenija Rossii i sopredel'nyh gosudarstv [Fossil flowering plants of Russia and adjacent countries]* (ed. by L. Budantsev). Izdatelstvo Nauka Leningradskoe otdnie, 1974., Leningrad.

Bonilla-Barbosa, J., Novelo, A., Hornelas Orozco, Y. & Márquez-Guzmán, J. (2000) Comparative seed morphology of Mexican Nymphaea species. *Aquat Bot*, 68, 189-204.

Crepet, W.L. & Nixon, K.C. (1998) Fossil Clusiaceae from the late Cretaceous (Turonian) of New Jersey and implications regarding the history of bee pollination. *Am J Bot*, 85, 1122-1133.

Drummond, A.J., Suchard, M.A., Xie, D. & Rambaut, A. (2012) Bayesian phylogenetics with BEAUti and the BEAST 1.7. *Mol Biol Evol*, 29, 1969-1973.

Ho, S.Y.W. & Phillips, M.J. (2009) Accounting for calibration uncertainty in phylogenetic estimation of evolutionary divergence times. *Syst Biol*, 58, 367-380.

Magallón, S. & Sanderson, M.J. (2001) Absolute diversification rates in angiosperm clades. *Evolution*, 55, 1762-1780.

Magallón, S., Crane, P.R. & Herendeen, P.S. (1999) Phylogenetic pattern, diversity, and diversification of Eudicots. *Ann Mo Bot Gard*, 86, 297-372.

Meseguer, A.S. & Sanmartín, I. (2012) Paleobiology of the genus *Hypericum* (Hypericaceae): a survey of the fossil record and its palaeogeographic implications. *An Jard Bot Madr*, 69, 97-106.

Meseguer, A.S., Aldasoro, J.J. & Sanmartin, I. (2013) Bayesian inference of phylogeny, morphology and range evolution reveals a complex evolutionary history in St. John's wort (*Hypericum*). *Mol Phylogenet Evol*, 67, 379-403.

Meseguer, A.S., Lobo, J.M., Ree, R.H., Beerling, D.J. & Sanmartin, I. (2015) Integrating fossils, phylogenies, and niche models into biogeography to reveal ancient evolutionary history: the case of *Hypericum* (Hypericaceae). *Syst Biol*, 64, 215-232.

Molnár V, A., Horváth, O., Tökölyi, J. & Somlyay, L. (2013) Typification and seed morphology of Elatine hungarica (Elatinaceae). *Biologia*, 68, 210-214.

Nürk, N.M., Madriñán, S., Carine, M.A., Chase, M.W. & Blattner, F.R. (2013) Molecular phylogenetics and morphological evolution of St. John's wort (*Hypericum*; Hypericaceae). *Mol Phylogenet Evol*, 66, 1-16.

Popiela, A., Łysko, A., Molnár V, A., Kącki, Z. & Lukács, B.A. (2015) Distribution, morphology and habitats of Elatine triandra (Elatinaceae) in Europe, with particular reference to the central part of the continent. *Acta Bot Gall*, 162, 325-337.

Robson, N.K.B. (1981) Studies in the genus *Hypericum* L. (Guttiferae). 2. Characters of the genus. *Bull. Brit. Mus. (Nat. Hist.), Bot.* , 8, 55–226.

Robson, N.K.B. (2012) Studies in the genus *Hypericum* L. (Hypericaceae) 9. Addenda, corrigenda, keys, lists and general discussion. *Phytotaxa*, 72, 1-111.

Ruhfel, B.R. (2011) *Systematics and biogeography of the clusioid clade (Malpighiales). PhD dissertation.* Harvard University, Cambridge, Massachusetts.

Ruhfel, B.R., Stevens, P.F. & Davis, C.C. (2013) Combined morphological and molecular phylogeny of the clusioid clade (Malpighiales) and the placement of the ancient rosid macrofossil *Paleoclusia*. *Int J Plant Sci*, 174, 910-936.

Ruhfel, B.R., Bove, C.P., Philbrick, C.T. & Davis, C.C. (2016) Dispersal largely explains the Gondwanan distribution of the ancient tropical clusioid plant clade. *Am J Bot*, 103, 1117-1128.

Ruhfel, B.R., Bittrich, V., Bove, C.P., Gustafsson, M.H.G., Philbrick, C.T., Rutishauser, R., Xi, Z. & Davis, C.C. (2011) Phylogeny of the clusioid clade (Malpighiales): Evidence from the plastid and mitochondrial genomes. *Am J Bot*, 98, 306-325.

Sanderson, M.J. & Doyle, J.A. (2001) Sources of error and confidence intervals in estimating the age of angiosperms from rbcL and 18S rDNA data. *Am J Bot*, 88, 1499-1516.

Xi, Z., Ruhfel, B.R., Schaefer, H., Amorim, A.M., Sugumaran, M., Wurdack, K.J., Endress, P.K., Matthews, M.L., Stevens, P.F., Mathews, S. & Davis, C.C. (2012) Phylogenomics and a posteriori data partitioning resolve the Cretaceous angiosperm radiation Malpighiales. *Proc Natl Acad Sci USA*, 109, 17519-17524.

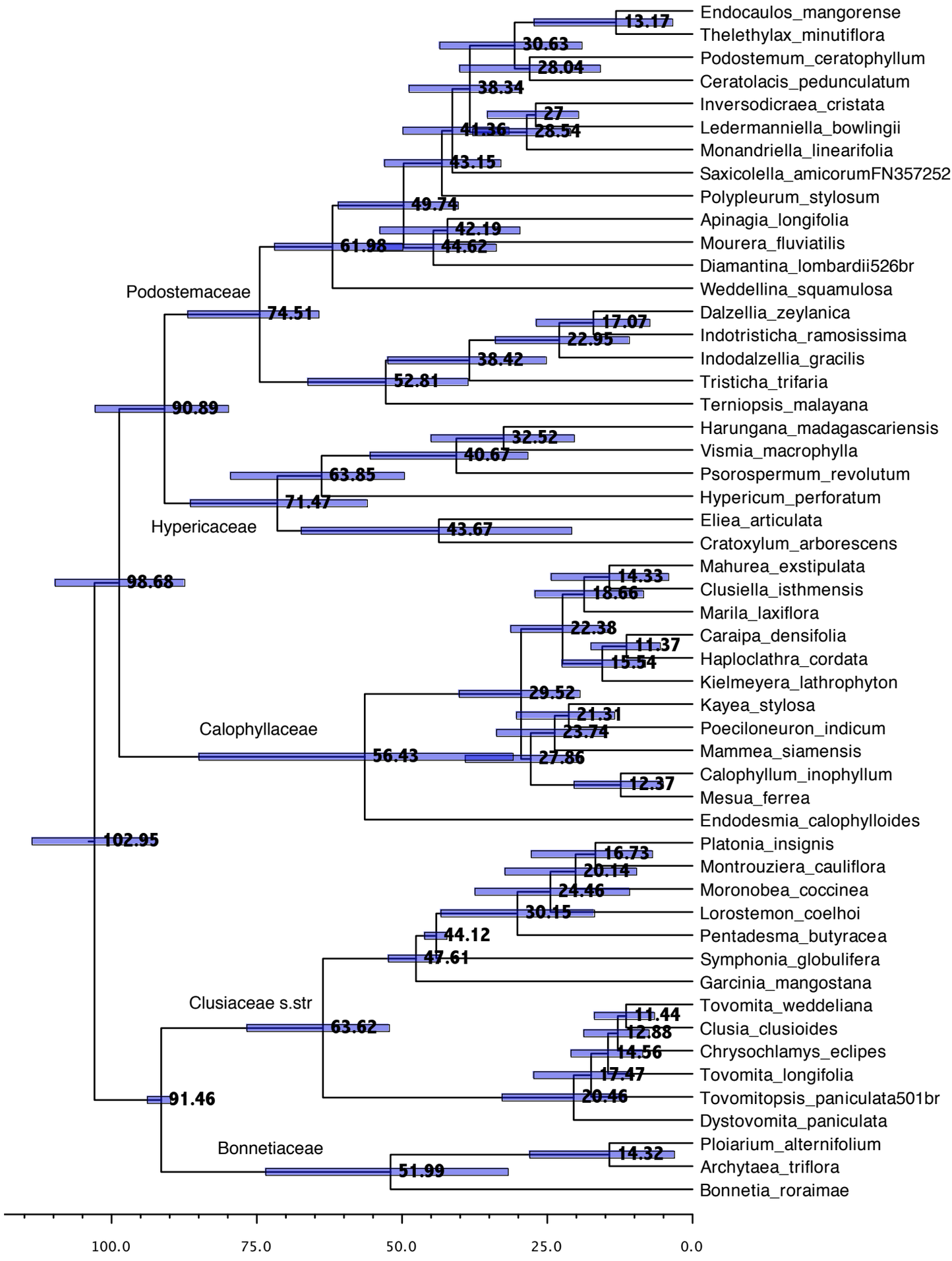

Fig. S1. Divergence time estimation analysis of the clusioid clade, using the BC position of fossil *Paleoclusia* (see Appendix S3 for an explanation). MCC tree from BEAST showing median divergence times and 95% HPD intervals derived from Ruhfel et al. (2011) multigene phylogeny

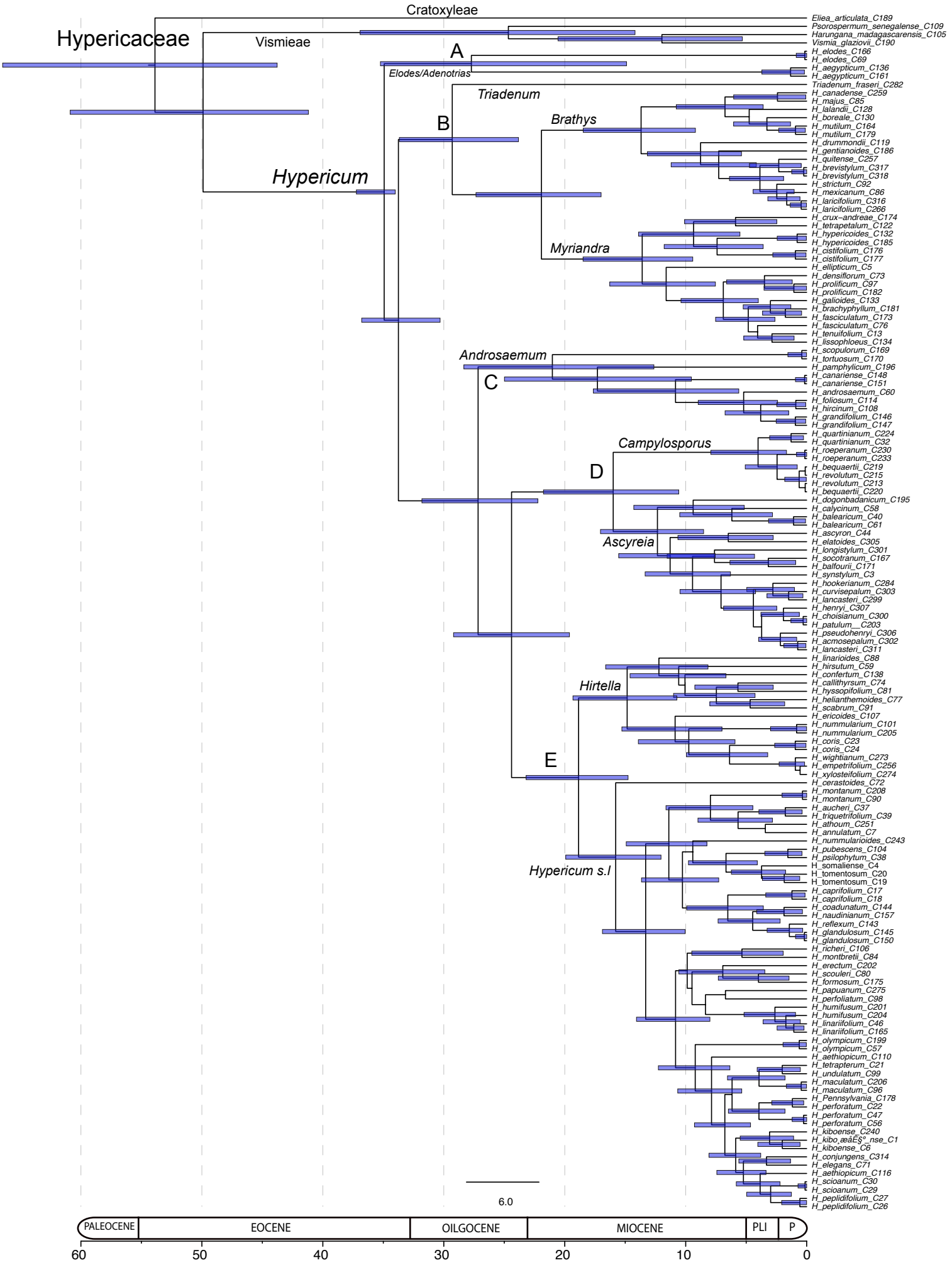

Fig. S2. Divergence time estimation analysis of *Hypericum* in BEAST. MCC (maximum clade credibility) tree showing median divergence times and 95% HPD (high posterior density) confidence intervals (for main lineages), derived from the concatenate dataset of Meseguer et al. (2015). Clade names represent major lineages recovered by Meseguer et al. (2013).

Figure S2

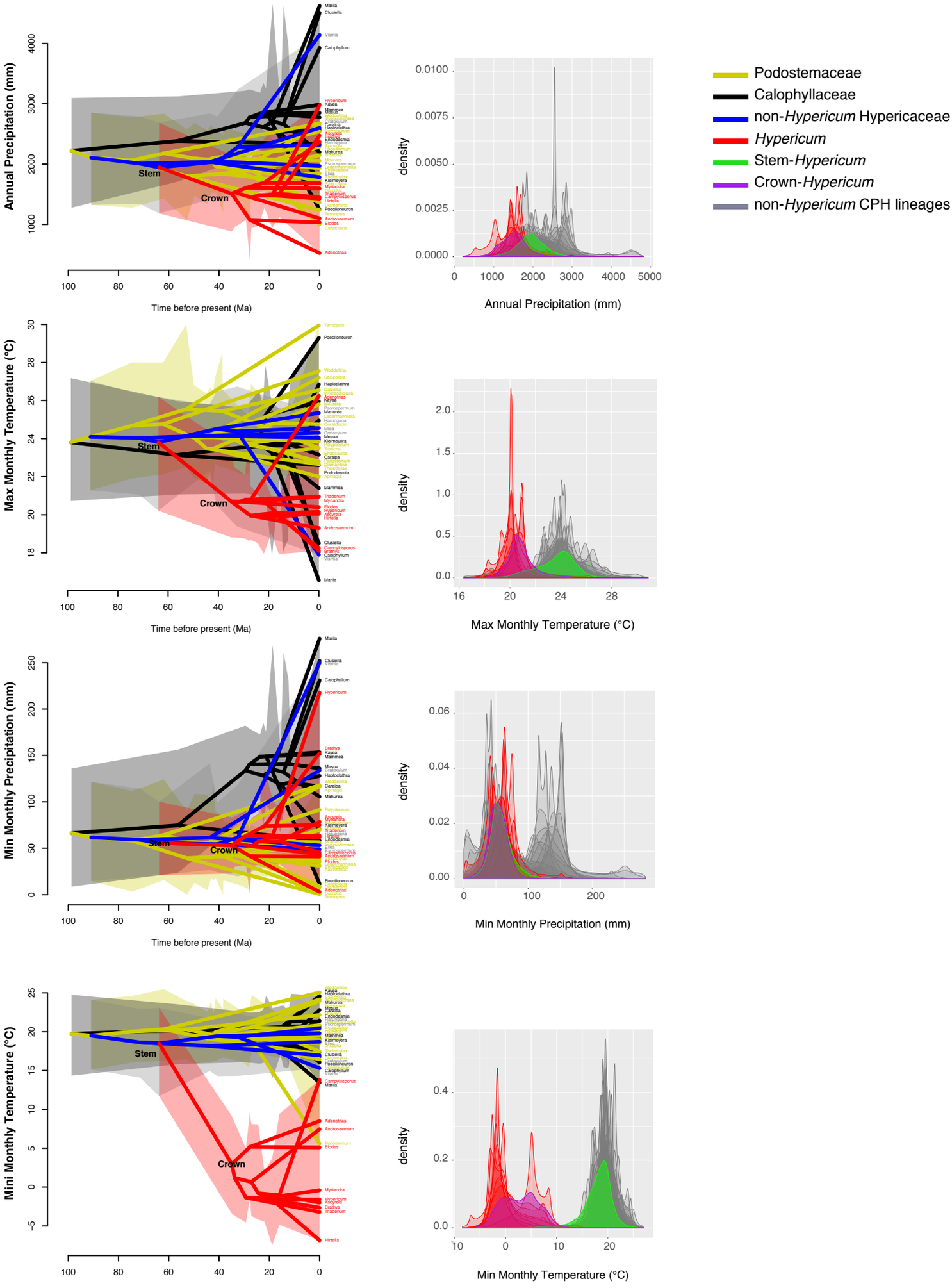

Fig. S3. Traitgrams showing the inferred evolution of climatic variables (Annual Precipitation, Min Monthly Precipitation, Min and Max Monthly Temperature), estimated without a fossil calibration, over the dated phylogenetic tree of the clusioid CPH clade in a space defined by the phenotype (y axis). Shaded areas encompass all HPD intervals of the group concerned. Right figure: Posterior distributions of ancestral traits estimated for each node in the tree.

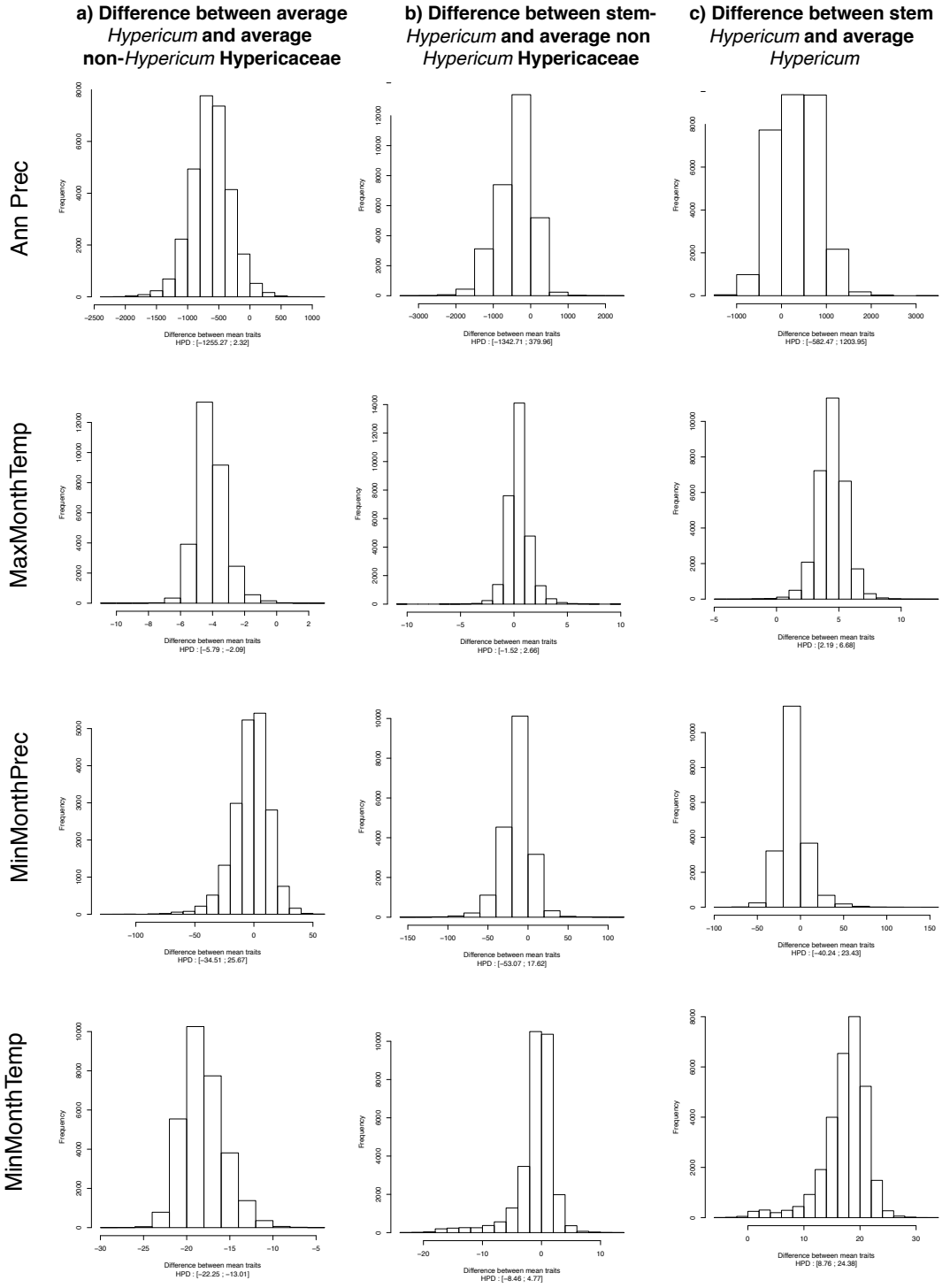

Fig. S4. Posterior distribution of the difference between estimated ancestral values using fossil information: **(a)** the average trait values estimated for all most recent common ancestors (mrca) of *Hypericum* clades (including crown node) and the average values estimated for the mrca of all other non-*Hypericum* Hypericaceae clades; **(b)** the values estimated for stem-*Hypericum* node and the average values estimated for the mrca of all other non-Hypericum Hypericaceae; **(c)** the average trait values estimated for all mrca of *Hypericum* clades (including crown node) and the values estimated for stem-*Hypericum* node; 95% highest posterior density (HPD) intervals larger/lower than 0 (positive/negative values) indicate higher/lower values for one group as compared to the other.

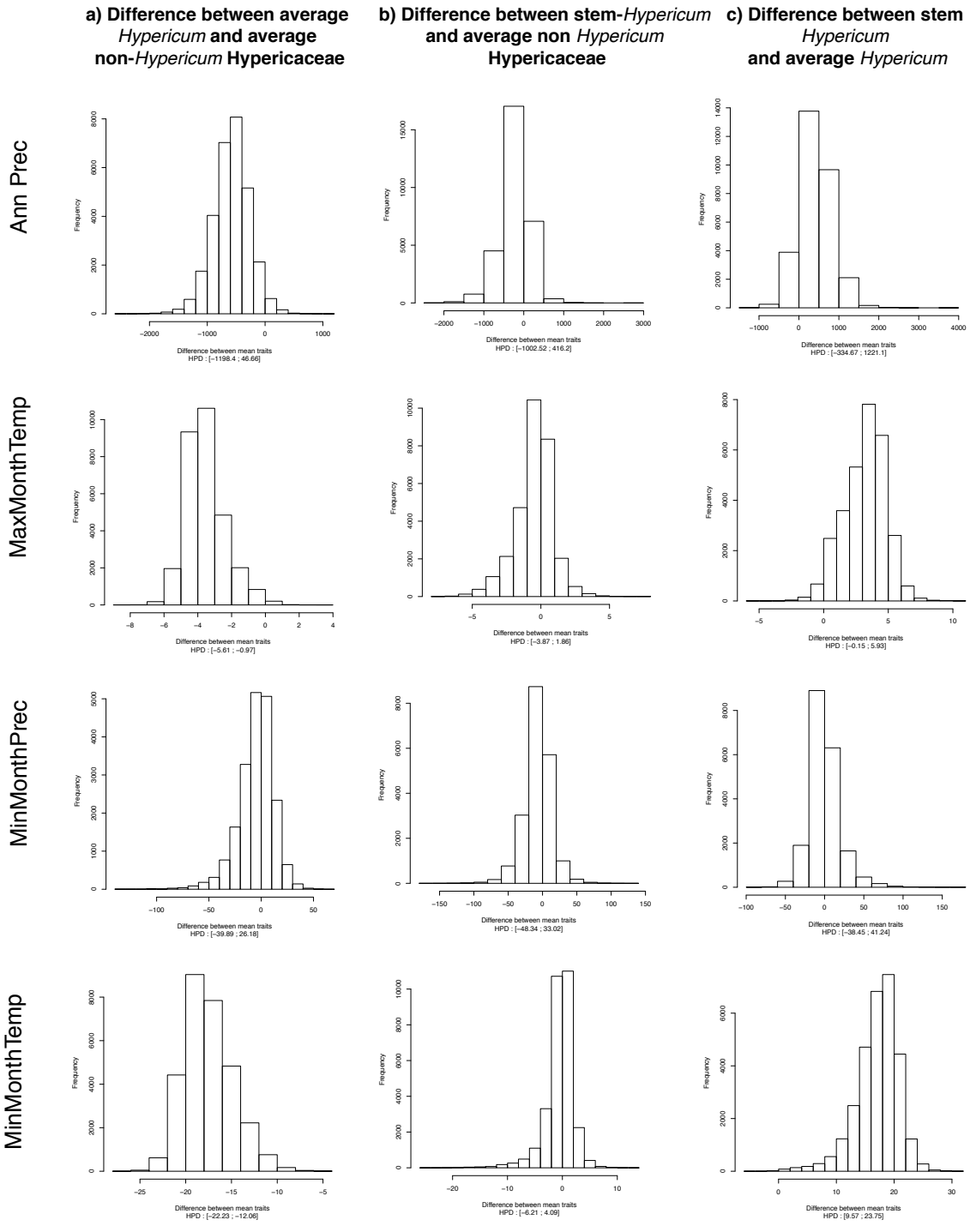

Fig. S5. Posterior distributions of the difference between ancestral values estimated in the tree without using fossil information: **(a)** the average trait values estimated for all most recent common ancestors (mrca) of *Hypericum* clades (including crown node) and the average values estimated for the mrca of all other non-*Hypericum* Hypericaceae clades; **(b)** the values estimated for stem-*Hypericum* node and the average values estimated for the mrca of all other non-Hypericum Hypericaceae; **(c)** the average trait values estimated for all mrca of *Hypericum* clades (including crown node) and the values estimated for stem-*Hypericum* node; 95% highest posterior density (HPD) intervals larger/lower than 0 (positive/negative values) indicate higher/lower values for one group as compared to the other.

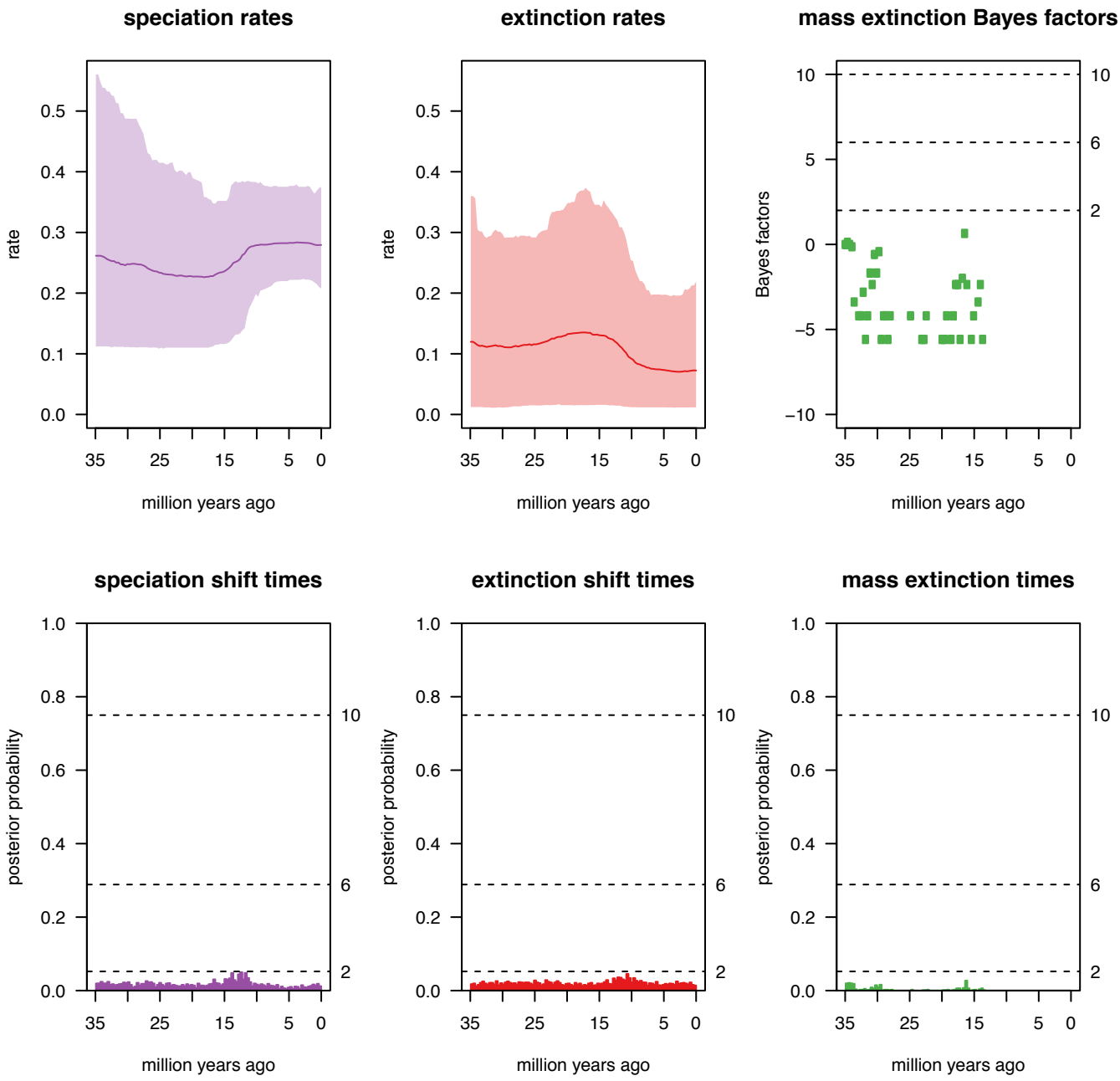

Fig. S6. Result of the CoMET analysis (TESS R package), showing the changes in speciation and extinction rates in the *Hypericum* clade through time along with the shift times for the evolutionary events. Ma, millions of years ago.

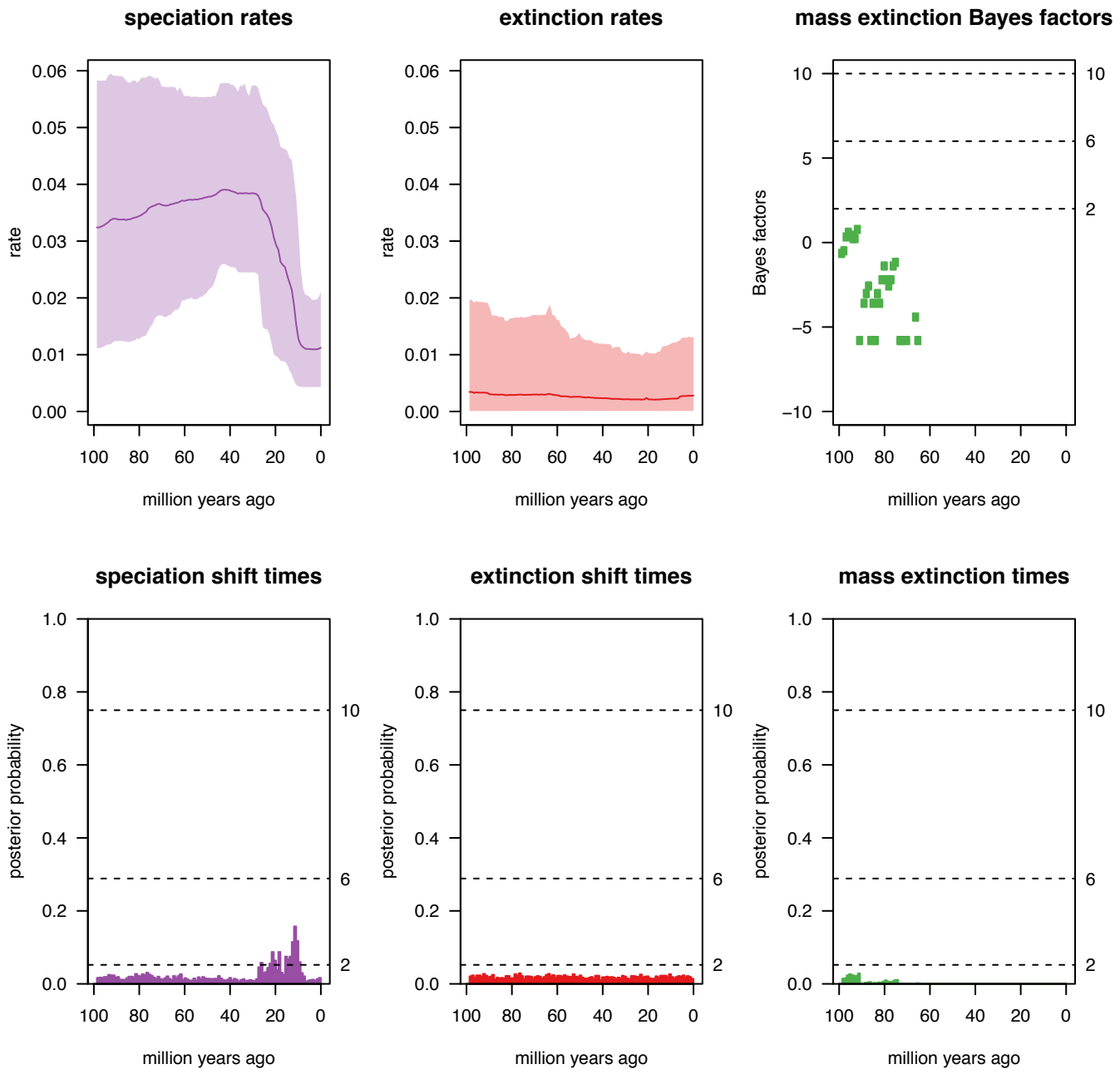

Fig. S7. Result of the CoMET analysis (TESS R package), showing the changes in speciation and extinction rates in the clusioid CPH clade through time along with the shift times for the evolutionary events. Ma, millions of years ago.

Appendix S5

Supporting Information Tables

Table 1. Hypericaceae phylogenetic clades with assigned species numbers considered in the analyses. When required, the assignment of non-sampled species to phylogenetic clades is explained. We did not find enough morphologic and/or phylogenetic criteria to assign 4 non-sampled Hypericaceae species (of the about 600 described in the family) to phylogenetic clades. Therefore, these species have not been considered in the analysis. Missing species correspond to Hypericeae genera *Lianthus* (1 sp.), *Thornea* (2 spp.) and *Santomasia* (1 sp.), which have been considered part of *Hypericum* (Ruhfel et al. 2011).

Phylogenetic clade	# sp.	Reference
Cratoxyleae	7	(APG 2001–; Stevens 2007b)
Harungana	2	(APG 2001–; Stevens 2007b)
Vismia	55	(APG 2001–; Stevens 2007b; Ruhfel et al. 2011)
Psorospermum	48	(APG 2001–; Stevens 2007b; Ruhfel et al. 2011)
Adenotrias	3	(Robson 2012)
Elodes	1	(Robson 2012)
Brathys+*Trigynobrathys*	147	This clade includes species from sections *Brathys* (88 spp) and *Trigynobrathys* (59 spp; (Robson 1987, 1990), which have been shown to be non-monophyletic (Meseguer et al. 2013; Nürk et al. 2013)
Myriandra	30	Robson 2012
Triadenum	6	Tropicos (http://www.tropicos.org)
Androsaemum+*Bupleuroides+ Webbia+ Arthrophyllum*	11	This clade includes sections *Androsaemum* (4spp), *Webbia* (1), *Arthrophyllum* (5), and *Bupleuroides* (1sp; (Robson 2012)) following Meseguer et al (2013) *Webbia* and *Arthrophyllum* are grouped together with *Androsaemum* because there were not enough occurrences on GBIF for this clade.
Triadenioides+*Sampsonia*	5	This group includes the section *Sampsonia* (2spp) and all the Socotran species of the section *Triadenioides** (3 spp), which form part of the same phylogenetic clade (Meseguer et al. 2013). The section *Triadenioides* has been shown to be polyphyletic, with the Socotran species *H. scopulorum* and *H.tortuosum* falling in a different clade than the continental species (Meseguer et al. 2013; Nürk et al. 2013). The non-sampled Socotran species from section *Triadenioides, H. fieriense,* were included in this clade as well, based on its geographic distribution.
Ascyreia+*Roscyna+Takasagoya+Psorophytum+Campylosporus+Umbraculoides*	64	This clade includes species from the non-monophyletic sections *Ascyreia* (50 spp.), *Psorophytum* (1sp), *Roscyna* (2spp.) and *Takasagoya* (5 spp.), as well as 5 spp. from section *Campylosporus**; *H. synstylum, dogonbandanicum, socotranum, balfouri and smithii* (Meseguer et al. 2013; Nürk et al. 2013). We also included the non-sampled section *Umbraculoides* (1spp) in this clade, as it is has been suggested to be closely related to *Ascyreia* (Robson 2012).
Campylosporus	7	This group is formed by the Afromontane species of the section *Campylosporus* as recovered by Meseguer et al (2013). The group also includes *H. lanceolatum* (Meseguer et al., in prep) and the non-sampled species *H. madagascariensis*, which has been suggested to be closely related to *H. lanceolatum* (Robson 1985). All these species share the following characters (synapomorphies): styles partly coherent, dark glands present and petals persistent. The non-sampled species *H.gnidifolium* was also assigned to this group, as has been suggested to be closely related to *H. roeperianum* (Robson 1985)
Hirtella+Coridium+Inodora+ Monanthema+Taeniocarpium+ Triadenioides	77	This clade includes the non-monophyletic sections *Hirtella* (30spp.), *Coridium* (6), *Inodora* (1), *Monanthema* (7spp.), *Taeniocarpium** (29spp.) and *Triadenioides** (4spp.) (Meseguer et al. 2013; Nürk et al. 2013). The section *Taeniocarpium* is polyphyletic with species located in 2 different clades in (Meseguer et al. 2013; Nürk et al. 2013)'s phylogenies. Although in these studies a few species of the morphologically defined section *Taeniocarpium* fall within the *Hypericum* group, most of them are part of the *Hirtella* group; therefore, we have included all species in this section within this clade. The continental species from section *Triadenioides**, *H. pallens, H. ternatum, H. musadoganii* and *H. haplophylloides* (Robson 2012), have also been included in this clade

		(see above).
Hypericum	144	This clade includes 13 non-monophyletic sections: *Hypericum* 44 spp, *Concinna* 1, *Graveolentia* 9, *Elodeoidea* 8, *Olympia* 4, *Drosocarpium* 11, *Oligostema* 6, *Thasia* 1, *Crossophyllum* 4, *Humifusoideum* 12, *Adenosepalum* 29 (Robson 2012), *Heterophylla* 1, *Origanifolia* 13, *Campylopus* 1. The last one has been grouped together with *Hypericum* because there were not enough occurrences on GBIF for this clade

Table 2. Clusioid phylogenetic clades with assigned species numbers considered in the analyses. When required, the assignation of non-sampled species to phylogenetic clades is explained.

Phylogen. clade	**# sp.**	**Reference**
Tristicha	1	(Ruhfel et al. 2011; Koi et al. 2012)
Dalzellia	5	(Ruhfel et al. 2011; Koi et al. 2012)
Indotristicha	2	(Ruhfel et al. 2011; Koi et al. 2012) # not included in the ENM analyse, not enough occurrences on GBIF
Indodalzellia	1	(Ruhfel et al. 2011; Koi et al. 2012) # not included in the ENM analyse, not enough occurrences on GBIF
Terniopsis	8	(Ruhfel et al. 2011; Koi et al. 2012)
Weddellina	1	(Ruhfel et al. 2011; Koi et al. 2012)
Diamantina	1	(Ruhfel et al. 2011; Koi et al. 2012)
Mourera	8	(Ruhfel et al. 2011; Koi et al. 2012)
Neotropical_Pod	113	The Neotrop_Pod clade includes 11 non-monophyletic genera: *Apinagia* 51spp, *Castelnavia* 5spp, *Jenmaniella* 7spp, *Lophogyme* 1spp, *Marathrum* 10spp (includes 1 *Vanroyenella* sp), *Monostylis* 1, *Noveloa* 2, *Oserya* 5, *Rhyncholacis* 22, *Wettsteiniola* 3, *Macarenia* 1, *Autana* 1spp (Ruhfel et al. 2011; Koi et al. 2012; Tippery et al. 2013).
Endocaulos*+ Paleodicraeia+ Sphaerothylax*	4	Phylogenetic evidence shows that the Madagascar genera *Endocaulos* and *Thelethylax* form a monophyletic group (Ruhfel et al. 2011; Koi et al. 2012). *Paleodicraeia* and *Sphaerothylax* are also distributed in Madagascar but they have not been sampled in previous phylogenetic works. We included the species of *Paleodicraeia* together with *Endocaulos* based on its geographic distribution but also on the presence of synapomorphic characters (increased rib number; (Moline et al. 2007; Thiv et al. 2009). We also included *Sphaerothylax* in this group, as species in this genus possess bilocular ovaries, a character that seems to be restricted to the endemic Malagasy genera *Endocaulos* and *Thelethylax*, as well as to *Saxicolella* pro parte (Ameka et al. 2002).
Thelethylax	2	(Koi et al. 2012)
Podostemum	11	(Ruhfel et al. 2011; Koi et al. 2012)
Saxicolella	2	*Saxicolella* is non monophyletic (Koi et al. 2012), with two species belonging to the group labelled (*Saxicolella* [Aulea]) in Ruhfel et al. ((2011)). The remaining 5 species of *Saxicolella* (*Saxicolella* s.s.) have been suggested to be likely represented by *Saxicolella nana* (Ruhfel et al. 2011), which is weakly supported as sister to the *Ledermaniella* s.l. clade in Ruhfel et al. ((2011))'s phylogeny.
Asian_Pod	70	This clade includes 15 non-monophyletic genera: *Cladopus* 9spp, *Farmeria* 1, *Griffithella* 1, *Hansenia* 2, *Hydrobryopsis* 1, *Hydrobryum* 23, *Hydrodiscus* 1, *Mafferia* 1, *Paracladopus* 2, *Polypleurum* 17, *Thawatchaia* 1, *Willisia* 2, *Zeylanidium* 5, *Diplobryum* 4spp (Ruhfel et al. 2011; Koi and Kato 2012; Koi et al. 2012).
Ceratolacis*+Cipoia*	4	These two genera are sister clades (Ruhfel et al. 2011; Koi et al. 2012)
Monandriella	1	(Ruhfel et al. 2011; Koi et al. 2012) # not included in the ENM analyse, not enough occurrences on GBIF
Inversodicraea	20	(Ruhfel et al. 2011; Koi et al. 2012)
Ledermanniella_sl	52	This clade includes 12 non-monophyletic genera: *Ledermanniella* 26spp, *Dicraeanthus* 2spp, *Djinga 1spp, Leiothylax 3spp, Letestuella 1spp, Macropodiella 6spp, Stonesia 5pp, Winklerella* 1spp, *Saxicollela s.s.* 4 spp. (Ruhfel et al. 2011; Koi et al. 2012). *Angolaea* and *Zehnderia* have not been sampled before but both share a gynophore with *Dicraeanthus* and *Leiothylax* (cf. (Cook and Rutishauser 2007)) from the *Ledermanniella* clade. *Butumia* (1 spp) can also be included in this clade, as it was described as similar to other *Saxicolella s.s.* species (Cook and Rutishauser 2007).
Vismia	54	(APG 2001–; Ruhfel et al. 2011)
Harungana	2	(APG 2001–; Ruhfel et al. 2011)
Psorospermum	49	(APG 2001–; Ruhfel et al. 2011)

Hypericum	500	(Ruhfel et al. 2011; Robson 2012; Meseguer et al. 2013; Nürk et al. 2013)
Eliea	1	(Stevens 2007b)
Cratoxylum	6	(Stevens 2007b)
Calophyllum	186	(Stevens 2007a)
Caraipa	28	(Stevens 2007a)
Clusiella	7	(Stevens 2007a)
Haploclathra	4	(Stevens 2007a)
Kayea	75	(Stevens 2007a)
Kielmeyera	47	(Stevens 2007a)
Mahurea*+Neotatea*	6	We included the 4 non-sampled spp. of *Neotatea* from the Neotropics together with the Neotropical genus *Mahurea* (2app.), following Notis ((Notis 2004)) and Ruhfel et al. ((Ruhfel et al. 2013)), who suggested *Neotatea* to be sister to *Mahurea* based on the shared presence of intruded axile placentae bordered by in-curled carpel walls and seeds with a vascularized wing that does not completely surround the seed. In addition, the Calophyllaceae phylogeny reflects a nice geographical structure, with the Neotropical clades *Caraipa*, *Kielmeyera*, *Haploclathra*, and *Mahurea* forming a monophyletic group (Ruhfel et al. 2011), and thus *Neotatea* might be included in the Neotropical clade.
Mammea	75	(Stevens 2007a)
Marila	40	(Stevens 2007a)
Mesua	5	(Stevens 2007a)
Poeciloneuron	3	(Stevens 2007a)
Endodesmia*+ Lebrunia*	2	This clade includes the African *Endodesmia* (1sp) and *Lebrunia* (1sp) as they belong to the same tribe Endodesmieae (Stevens 2007a)
Clusia	300	(Stevens 2007a)
Chrysochlamys	55	(Stevens 2007a)
Tovomita	24	(Stevens 2007a)
Tovomita weddeliana	1	(Stevens 2007a)
Tovomitopsis	3	(Stevens 2007a)
Dystovomita	4	(Stevens 2007a)
Garcinia	260	(Stevens 2007a)
Montrouziera	5	(Stevens 2007a)
Platonia	1	(Stevens 2007a)
Moronobea	7	(Stevens 2007a)
Lorostemon+ Thysanostemon	7	*Thysanostemon* (2spp) may be closely related to *Lorostemon* (5 spp) (Ruhfel et al. 2011; Ruhfel et al. 2013). These two genera have very elongated flower buds and pollen with supratectal elements, features not present in other Symphonieae (Maguire 1964; Seetharam 1985)
Pentadesma	5	(Stevens 2007a)
Symphonia	23	(Stevens 2007a)
Archytaea	2	(APG 2001–; Weitzman et al. 2007)
Bonnetia	30	(APG 2001–; Weitzman et al. 2007)
Ploiarium	3	(APG 2001–; Weitzman et al. 2007)

Table 3. Climatic conditions in which Eocene–Oligocene *Hypericum* fossils occurred in the Eocene (560ppm) simulation. Abbreviations: AP = Annual precipitation; MXMT = Maximum monthly temperature; MNMP = Minimum monthly precipitation; MNMT= Minimum monthly temperature.

AP min	AP max	MXMT min	MXMT max	MNMP min	MNMP max	MNMT min	MNMT max
809.07	1293.72	20.48	30.73	27.15	52.26	-5.72	10.06

Table 4. Present climatic values of every major clade (tip) in the clusioid CPH tree for selected variables. Abbreviations: Abbreviations: AP = Annual precipitation; MXMT = Maximum monthly temperature; MNMP = Minimum monthly precipitation; MNMT= Minimum monthly temperature.

	AP min	MXMT min	MNMP min	MNMT min	AP max	MXMT max	MNMP max	MNMT max
Adenotrias	57	20.1	0	3.5	990	32.4	6	13.5
Androsaemum	109	10.5	0	-7.1	2092	28.1	87	22
Apinagia	388	13.6	0	10.3	4205	30.4	233	27.7
Ascyreia	57	6.6	0	-29.3	4892	33.6	157	25.3
Brathys	8	3.6	0	-32.1	4730	32.6	305	26.8
Calophyllum	306	5.1	0	4.4	7548	31	462	27.7
Campylosporus	260	7.1	0	3.2	2639	29.4	91	24.4
Caraipa	832	16.1	0	15.3	4293	30.2	233	27.4
Ceratolacis	459	21.4	1	15.8	1550	27.2	17	23.3
Clusiella	852	8.8	4	8.1	8167	28.2	500	26.6
Cratoxylum	795	17.6	0	7	4407	30.5	268	26.9
Dalzellia	1540	25.1	2	16.2	1769	28	3	22.8
Diamantina	1177	21.4	5	15.8	1550	23.9	11	18.5
Eliea	566	21.6	13	14.6	3000	27	93	22.8
Elodes	423	14.1	1	-1.1	1646	26.7	81	11.3
Endocaulos	1137	18.2	1	15.4	2555	28.8	69	24.1
Endodesmia	1537	17.4	1	16.4	3125	27.8	115	25.1
Haploclathra	1606	25.4	30	22.2	3484	28.3	226	26.9
Harungana	612	16.1	0	13.2	4022	33	124	27.7
Hirtella	57	6.5	0	-32.4	2797	33.6	124	18.7
Hypericum	6	6.4	0	-29.3	5950	33.9	435	26.1
Inversodicraea	2326	25.7	40	23.5	2956	26.8	70	24.4
Kayea	1890	24.4	59	23.3	4080	27.5	248	25.9
Kielmeyera	538	17.7	0	11.1	2934	30.2	141	26.8
Ledermanniella	910	19.5	0	15.8	2957	30	76	24.8
Mahurea	914	19.8	5	18.6	3484	30.1	206	27
Mammea	18	13.6	0	11.5	5679	29.2	303	26.6
Marila	625	3.7	0	-1.2	8623	29.4	552	28.1
Mesua	1330	19.4	4	16.6	4224	28.5	268	26.3
Mourera	678	22.8	2	15.2	3436	28.8	111	26.5
Myriandra	442	12.5	2	-23.8	2929	29.4	148	23
Podostemum	826	17.2	2	-13.8	3750	28.4	139	25
Poeciloneuron	1131	25	7	16.1	1355	33.6	16	17.5
Polypleurum	882	20.2	4	8.8	4204	27.5	179	24.1
Psorospermum	428	17.7	0	11.9	3512	33	97	27.7
Saxicollela	1473	27.2	19	23.8	1987	27.2	43	24.5
Terniopsis	1088	29.2	0	21.4	1386	30.7	1	22.9

Thelethylax	784	19.1	2	12.4	2705	26.2	83	22.5
Triadenum	442	12.4	12	-23.8	2752	29.5	115	17.4
Tristicha	459	16.3	0	10.7	3833	30.7	139	26.3
Vismia	118	5.7	0	2.5	8167	30.1	500	28.1
Weddellina	1804	25.1	3	23.3	3547	30	233	26.8

Table 5. Bayes Factor comparisons (2 ln BF) of all possible combinations of the 6 candidate branching-process models of *Hypericum* diversification based on marginal likelihood calculations using steeping stone simulations. The constant-rate birth-death process (*ConstBD*), the episodic model (*EpisodicBD*) and the four different continuous-varying rate models: *DecrB* – a process where extinction rate remains constant, but speciation decreases through time. *IncrB* – extinction remains constant, but speciation increases through time. *DecrD* –speciation remains constant, but extinction decreases through time. *IncrD* – speciation remains constant, but extinction increases through time.

M0	**M1**	**BF**
EpisodicBD	DecrB	19.628911
ConstBD	DecrB	18.336460
EpisodicBD	IncrD	13.356410
IncrB	DecrB	13.061098
ConstBD	IncrD	12.063959
DecrD	DecrB	9.892310
EpisodicBD	DecrD	9.736600
ConstBD	DecrD	8.444149
IncrB	IncrD	6.788597
EpisodicBD	IncrB	6.567813
IncrD	DecrB	6.272501
ConstBD	IncrB	5.275362
DecrD	IncrD	3.619810
IncrB	DecrD	3.168787
EpisodicBD	ConstBD	1.292451
ConstBD	ConstBD	0.000000
DecrB	DecrB	0.000000
DecrD	DecrD	0.000000
IncrB	IncrB	0.000000
IncrD	IncrD	0.000000
EpisodicBD	EpisodicBD	0.000000
ConstBD	EpisodicBD	-1.292451
DecrD	IncrB	-3.168787
IncrD	DecrD	-3.619810
IncrB	ConstBD	-5.275362
DecrB	IncrD	-6.272501

IncrB	EpisodicBD	-6.567813
IncrD	IncrB	-6.788597
DecrD	ConstBD	-8.444149
DecrD	EpisodicBD	-9.736600
DecrB	DecrD	-9.892310
IncrD	ConstBD	-12.063959
DecrB	IncrB	-13.061098
IncrD	EpisodicBD	-13.356410
DecrB	ConstBD	-18.336460
DecrB	EpisodicBD	-19.628911

Table 6. Bayes Factor comparisons (2 ln BF) of all possible combinations of the 6 candidate branching-process models of clusioid CPH diversification based on marginal likelihood calculations using steeping stone simulations. The constant-rate birth-death process (*ConstBD*), the episodic model (*EpisodicBD*) and the four different continuous-varying rate models: *DecrB* – a process where extinction rate remains constant, but speciation decreases through time. *IncrB* – extinction remains constant, but speciation increases through time. *DecrD* –speciation remains constant, but extinction decreases through time. *IncrD* – speciation remains constant, but extinction increases through time.

M0	**M1**	**BF**
ConstBD	DecrD	18.0044239
IncrD	DecrD	16.7940719
ConstBD	IncrB	15.8694419
EpisodicBD	DecrD	15.8094652
IncrD	IncrB	14.6590899
ConstBD	DecrB	13.8732203
EpisodicBD	IncrB	13.6744833
IncrD	DecrB	12.6628683
EpisodicBD	DecrB	11.6782617
DecrB	DecrD	4.1312036
ConstBD	EpisodicBD	2.1949587
IncrB	DecrD	2.1349820
DecrB	IncrB	1.9962216
ConstBD	IncrD	1.2103520
IncrD	EpisodicBD	0.9846066
ConstBD	ConstBD	0.0000000
DecrB	DecrB	0.0000000
DecrD	DecrD	0.0000000
IncrB	IncrB	0.0000000
IncrD	IncrD	0.0000000
EpisodicBD	EpisodicBD	0.0000000

EpisodicBD	IncrD	-0.9846066
IncrD	ConstBD	-1.2103520
IncrB	DecrB	-1.9962216
DecrD	IncrB	-2.1349820
EpisodicBD	ConstBD	-2.1949587
DecrD	DecrB	-4.1312036
DecrB	EpisodicBD	-11.6782617
DecrB	IncrD	-12.6628683
IncrB	EpisodicBD	-13.6744833
DecrB	ConstBD	-13.8732203
IncrB	IncrD	-14.6590899
DecrD	EpisodicBD	-15.8094652
IncrB	ConstBD	-15.8694419
DecrD	IncrD	-16.7940719
DecrD	ConstBD	-18.0044239

Appendices S7–S14. Ancestral climatic reconstruction of the different variables. Median and HPD limits for the sigma parameter of each branch and for the ancestral trait estimated for every node. Numbers correspond with the numbers on the figure bellow.

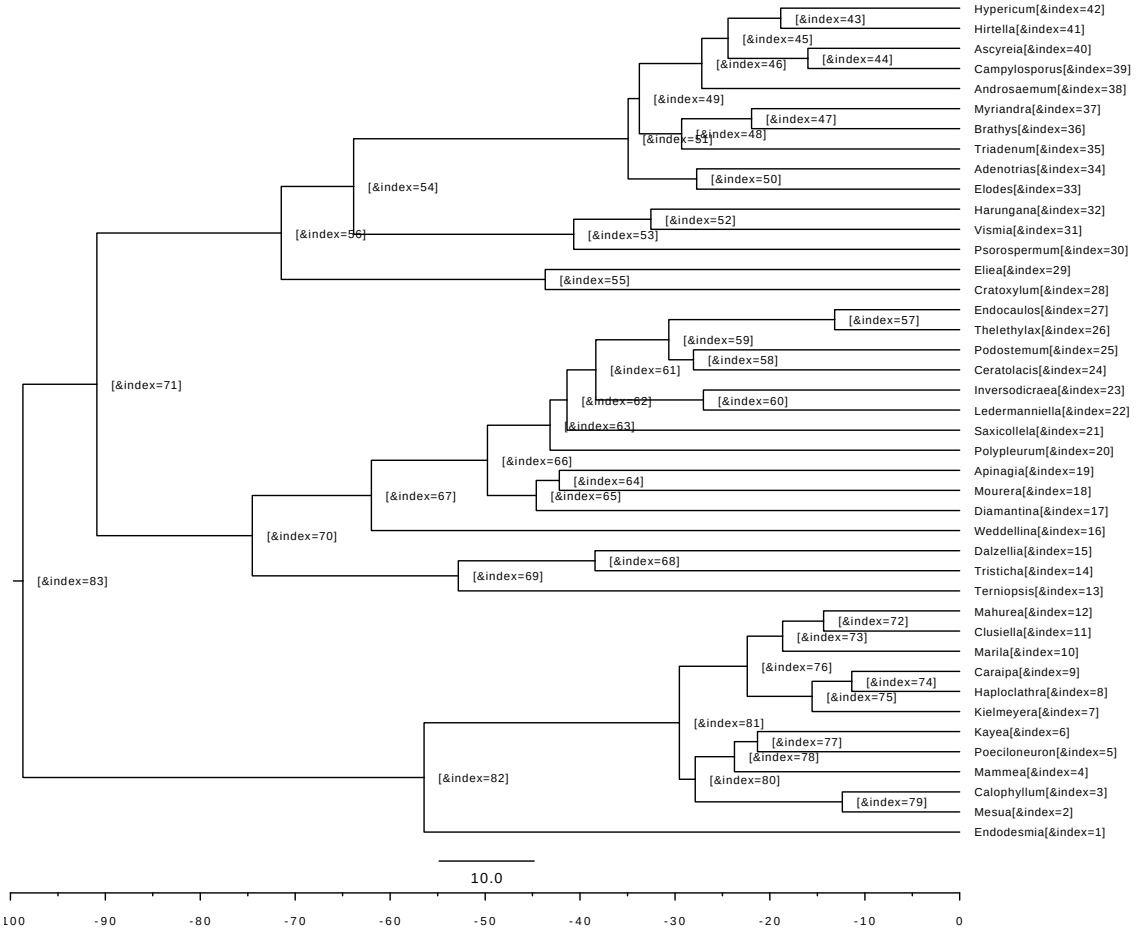

REFERENCES

Ameka, K. G., E. Pfeifer, and R. Rutishauser. 2002. Developmental morphology of *Saxicolella amicorum* and *S. submersa* (Podostemaceae: Podostemoideae) from Ghana. Bot. J. Linn. Soc. 139:255–273.

APG. 2001–. Angiosperm phylogeny website.

Cook, C. D. K. and R. Rutishauser. 2007. Podostemaceae. Pp. 304 – 344 *in* K. Kubitzki, ed. The families and genera of vascular plants. Flowering plants. Eudicots: Berberidopsidales, Buxales, Crossosomatales, Fabales p.p., Geraniales, Gunnerales, Myrtales p.p., Proteales, Saxifragales, Vitales, Zygophyllales, Clusiaceae alliance, Passifl oraceae alliance, Dilleniaceae, Huaceae, Picramniaceae, Sabiaceae, Springer-Verlag, Berlin, Germany.

Koi, S. and M. Kato. 2012. A taxonomic study of Podostemaceae subfamily Podostemoideae of Laos with phylogenetic analyses of *Cladopus*, *Paracladopus* and *Polypleurum*. Kew Bull. 67:331–365.

Koi, S., Y. Kita, Y. Hirayama, R. Rutishauser, K. A. Huber, and M. Kato. 2012. Molecular phylogenetic analysis of Podostemaceae: implications for taxonomy of major groups. Bot. J. Linn. Soc. 169:461–492.

Maguire, B. 1964. The botany of the Guyana highland— part V. Mem. N. Y. Bot. Gard. 10:1–278.

Meseguer, A. S., J. J. Aldasoro, and I. Sanmartin. 2013. Bayesian inference of phylogeny, morphology and range evolution reveals a complex evolutionary history in St. John's wort (*Hypericum*). Mol. Phylogenet. Evol. 67:379-403.

Moline, P., M. Thiv, G. K. Ameka, J. P. Ghogue, E. Pfeifer, and R. Rutishauser. 2007. Comparative morphology and molecular systematics of African Podostemaceae-Podostemoideae, with emphasis on *Dicraeanthus* and *Ledermanniella* from Cameroon. Int. J. Plant Sci. 168:159–180.

Notis, C. 2004. Phylogeny and character evolution of Kielmeyeroideae (Clusiaceae) based on molecular and morphological data. University of Florida, Gainesville.

Nürk, N. M., S. Madriñán, M. A. Carine, M. W. Chase, and F. R. Blattner. 2013. Molecular phylogenetics and morphological evolution of St. John’s wort (*Hypericum*; Hypericaceae). Mol. Phylogenet. Evol. 66:1-16.

Robson, N. K. B. 1985. Studies in the genus *Hypericum* L. (Guttiferae). 3. Sections 1. *Campylosporus* to 6a. *Umbraculoides*. Bull. Brit. Mus. (Nat. Hist.), Bot. 12:163–211.

Robson, N. K. B. 1987. Studies in the genus *Hypericum* L. (Guttiferae). 7. Section 29. *Brathys* (part 1). Bull. Brit. Mus. (Nat. Hist.), Bot. 16:1–106.

Robson, N. K. B. 1990. Studies in the genus *Hypericum* L. (Guttiferae). 8. Sections 29. *Brathys* (part 2) and 30. *Trigynobrathys*. Bull. Brit. Mus. (Nat. Hist.), Bot. 20:1–151.

Robson, N. K. B. 2012. Studies in the genus *Hypericum* L. (Hypericaceae) 9. Addenda, corrigenda, keys, lists and general discussion. Phytotaxa 72:1-111.

Ruhfel, B. R., V. Bittrich, C. P. Bove, M. H. G. Gustafsson, C. T. Philbrick, R. Rutishauser, Z. Xi, and C. C. Davis. 2011. Phylogeny of the clusioid clade (Malpighiales): Evidence from the plastid and mitochondrial genomes. Am. J. Bot. 98:306-325.

Ruhfel, B. R., P. F. Stevens, and C. C. Davis. 2013. Combined morphological and molecular phylogeny of the clusioid clade (Malpighiales) and the placement of the ancient rosid macrofossil *Paleoclusia*. Int. J. Plant Sci. 174:910-936.

Seetharam, Y. N. 1985. Clusiaceae: Palynology and systematics, Pondichéry, India.

Stevens, P. F. 2007a. Clusiaceae-Guttiferae *in* K. Kubitzki, ed. The families and genera of vascular plants. Springter, Berlin, Heidelberg.

Stevens, P. F. 2007b. Hypericaceae. Pp. 194–201 *in* K. Kubitzki, ed. The families and genera of vascular plants. Springer, Berlin, Heidelberg.

Thiv, M., J. P. Ghogue, V. Grob, K. Huber, E. Pfeifer, and R. Rutishauser. 2009. How to get off the mismatch at the generic rank in African Podostemaceae? . Plant Syst. Evol. 283:57–77.

Tippery, N. P., C. T. Philbrick, C. P. Bove, and D. H. Les. 2013. Systematics and phylogeny of neotropical Podostemaceae. Syst. Bot.

Weitzman, A. L., K. Kubitzki, and P. F. Stevens. 2007. Bonnetiaceae *in* K. Kubitzki, ed. The families and genera of vascular plants. Flowering plants. Eudicots: Berberidopsidales, Buxales, Crossosomatales, Fabales p.p., Geraniales, Gunnerales, Myrtales p.p., Proteales, Saxifragales, Vitales, Zygophyllales, Clusiaceae alliance, Passifl oraceae alliance, Dilleniaceae, Huaceae, Picramniaceae, Sabiaceae. Springer, Verlag, Berlin, Germany.